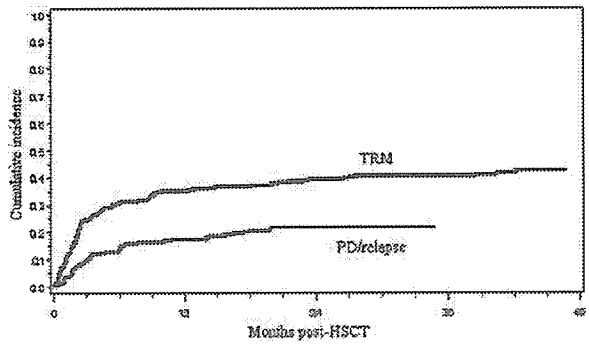

Figure 1. Cumulative incidences of treatment-related mortality (TRM) and disease relapse/progression (PD/relapse).

these died of GVHD (6 acute, 5 chronic) itself. The 14 factors shown in Table 3 were assessed with regard to their relation to TRM. A univariate analysis revealed that 6 factors, including older patient age, chemoresistant disease, prior autograft, prior radiotherapy, aggressive lymphoma other than PTCL, and chronic GVHD, were associated with a significantly increased risk of TRM. In a multivariate analysis using a logistic model, chemoresistant disease, prior autograft, and chronic GVHD remained significant.

The cumulative incidence of relapse and PD is shown in Figure 1. Relapse or progression of lymphoma after allo-HSCT was observed in 49 patients (21%; 5 indolent, 19 aggressive, 25 LBL), and 32 (14%; 3 indolent, 13 aggressive, and 16 LBL) died of PD. Of the 105 patients with chemoresistant disease before allo-HSCT, 61 (58%) died of treatment-related complications, 19 (18%) died of PD, and 25 (24%) are alive with a median follow-up of 20.9 months (range, 1.8-136.0 months). Of the 128 patients with chemosensitive disease before allo-HSCT, 37 (29%) died of treatment-related complications, 12 (9%) died of PD, and 79 (62%) are alive with a median follow-up of 35.2 months (range, 4.4-140.2 months). Eight (16%) of the 49 patients who showed PD died of treatment-related complications such as infection (n = 4), interstitial pneumonitis (n = 3), and GVHD (n = 1). Only 6 of the 70 patients who had passed 2 years after transplantation developed relapse thereafter.

Donor lymphocyte infusion

Donor lymphocyte infusions (DLIs) were given after the withdrawal of immunosuppressive therapy to those who relapsed or showed evidence of disease progression or persistent disease without any sign of GVHD. A total of 7 patients, including 5 with T-LBL, received DLI after allo-HSCT from an HLA-matched related donor (n = 6) or a -matched unrelated donor (n = 1). Two patients who received DLI from an HLA-matched related donor developed grade II acute GVHD, which subsequently extended to extensive chronic GVHD; one of them with T-LBL died without a response, whereas the other with T-cell lymphoma is still alive without disease progression 3.8 years after allo-HSCT. Five patients did not develop GVHD following DLI; 3 patients subsequently died of disease progression, but 2 patients with T-LBL are still alive without disease progression at 361 and 783 days after allo-HSCT.

OS and PFS

One hundred four (45%) of the 233 patients are currently alive with a median follow-up of 31 months (range, 1.8-138 months). The OS and PFS are, respectively, 45% and 40% at 2 years, and 39% and 36% at 5 years after allo-HSCT (Figure 2). Median OS and PFS are, respectively, 15.6 months (95% confidence interval, 9.6-27.6 months) and 9.6 months (6-18 months). The 2-year OS of those with indolent, aggressive, and lymphoblastic lymphoma was, respectively, 57%, 42%, and 41%. Patients with indolent lymphoma tended to have a better survival ($P = .131$, log rank test; $P = .064$, G. Wilcoxon test) (Figure 3). Kaplan-Meier estimates of OS of patients with 4 histologic subtypes of aggressive lymphoma, including diffuse large B-cell lymphoma (n = 44), PTCL (n = 22), extranodal NK/T-cell lymphoma, nasal type (n = 19), and others (n = 26), are shown in Figure 4.

The 14 clinical factors shown in Table 4 were assessed with regard to their relation to OS. A univariate analysis revealed that 5 factors, including chemoresistant disease, prior autograft, prior radiotherapy, aggressive lymphoma other than PTCL, and clinical subtype (aggressive versus indolent), were associated with a significantly worse OS. In a multivariate analysis using Cox proportional hazard models, chemoresistant disease, prior autograft, and prior radiotherapy were associated with a worse OS (Table 4). Acute GVHD, which was treated as a time-dependent variable, was not a significant factor for OS in both univariate and multivariate models. The relation between OS and response to chemotherapy is shown in Figure 5.

Discussion

This report describes the general outcome of patients with NHL who underwent modern allo-HSCT with a myeloablative regimen

Table 2. Causes of treatment-related mortality

Causes of TRM	Patients, no. (%)	No. of patients with GVHD	No. of patients without GVHD	Early death, no.*
GVHD	11 (11)			
Infection	29 (30)	15	8	6
Interstitial pneumonitis	16 (17)	15	0	1
Venoocclusive disease	11 (11)	5	4	2
Thrombotic microangiopathy	8 (8)	7	1	0
Heart failure	7 (7)	3	1	3
Hemorrhage	4 (4)	3	1	0
Renal failure	3 (3)	2	1	0
Others†	9 (9)	6	1	2
Total	98 (100)	56	17	14

GVHD indicates graft-versus-host disease.

*Early death was defined as treatment-related death before engraftment.

†Others (n = 9) were acute respiratory distress syndrome (n = 2), hepatic failure (n = 2), leukoencephalopathy (n = 1), secondary solid cancer (n = 1), suicide (n = 1), and unknown cause (n = 2).

Table 3. Univariate and multivariate analyses of treatment-related mortality

Variable	No.	Univariate analysis		Multivariate analysis	
		Hazard ratio (95% CI)	P	Hazard ratio (95% CI)	P
Age at transplantation			.035		—
Younger than 40 y	158	1.00		—	
40 y or older	75	1.82 (1.04-3.17)		—	
Clinical subtype			.349		—
Indolent	38	1.00		—	
Lymphoblastic	84	1.47 (0.66-3.32)		—	
Clinical subtype			.103		—
Indolent	38	1.00		—	
Aggressive	111	1.91 (0.88-4.16)		—	
Aggressive lymphoma			.045		—
PTCL	22	1.00		—	
Non-PTCL	89	2.85 (1.02-7.94)		—	
Response to chemotherapy			< .001		< .001
Sensitive	128	1.00		1.00	
Resistant	105	3.41 (1.97-5.88)		2.95 (1.66-5.25)	
Prior autograft			< .001		< .001
No	193	1.00		1.00	
Yes	40	4.74 (2.23-10.07)		4.09 (1.85-9.04)	
Prior radiotherapy			.010		—
No	152	1.00		—	
Yes	81	2.05 (1.18-3.55)		—	
Years of transplantation			.225		—
1996-2001	187	1.00		—	
1990-1995	46	1.49 (0.78-2.86)		—	
Donor			.295		—
HLA-matched	197	1.00		—	
HLA-mismatched	36	1.46 (0.72-2.98)		—	
HLA-matched donor			.437		—
Related	154	1.00		—	
Unrelated	43	1.24 (0.72-2.15)		—	
Source of stem cells*			.544		—
BM	159	1.00		—	
PBSCs	70	1.09 (0.82-1.46)		—	
Conditioning regimen			.144		—
TBI-containing	193	1.00		—	
Others	40	1.67 (0.84-3.30)		—	
GVHD prophylaxis†			.169		—
Cyclosporin + methotrexate	204	1.00		—	
Tacrolimus + methotrexate	22	1.86 (0.77-4.51)		—	
Acute GVHD			.537		—
No	78	1.00		—	
Yes	155	1.19 (0.69-2.06)		—	
Chronic GVHD			< .001		.029
No	79	1.00		1.00	
Yes	154	2.76 (1.53-4.98)		2.02 (1.07-3.77)	

CI indicates confidence interval; PTCL, peripheral T-cell lymphoma; HLA, human leukocyte antigen; BM, bone marrow; GVHD, graft-versus-host disease; and —, not applicable.

*Those who received cord blood (n = 2) or BM + PBSC (n = 2) were excluded because of the small number of patients.

†Seven patients using other GVHD prophylaxis were excluded.

in Japan, focusing on the background problems of myeloablative therapy and the identification of risk factors for TRM and OS. We showed that long-term, lymphoma-free survival could be achieved in approximately 40% of patients. Patients with FL had a better prognosis, consistent with previous reports.[8,10] Even in patients with aggressive lymphoma or LBL, long-term survival of 35% was identified, consistent with previous reports.[8,9] However, there were no significant differences between clinical subtypes (eg, aggressive versus indolent or PTCL versus non-PTCL) in a multivariate analysis. Because rituximab became commercially available after 2001 in Japan, patients with B-cell NHL who received anti-CD20 antibody therapy were not included in this study. The clinical effect of the introduction of rituximab on outcome after allogeneic transplantation should be carefully evaluated in a future study.

Our study confirmed a high TRM rate (42%) after conventional allo-HSCT with a myeloablative regimen, consistent with previous reports.[4-8,25] One of the major causes of death was severe regimen-related toxicities, which included interstitial pneumonitis, venoocclusive disease, cardiac and renal toxicity, and organ hemorrhage. Although TBI-based regimens are frequently chosen because lymphoma cells are considered to be sensitive to irradiation, they have also been associated with long-term complications, including

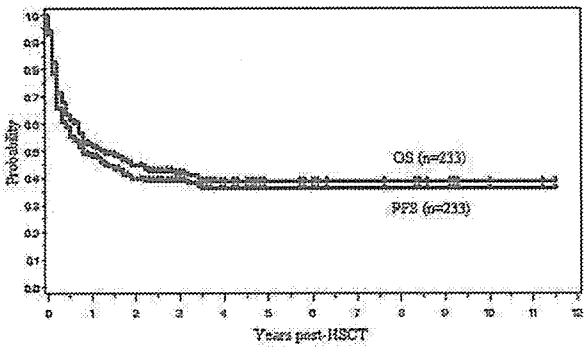

Figure 2. Overall survival (OS) and progression-free survival (PFS) for all 233 patients.

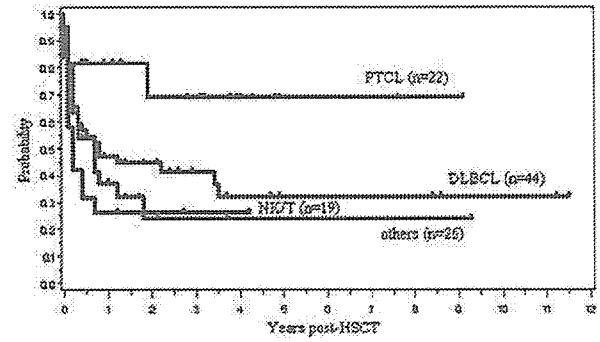

Figure 4. Overall survival for patients with 4 histologic subtypes of aggressive lymphoma. PTCL indicates peripheral T-cell lymphoma, unspecified; DLBCL, diffuse large B-cell lymphoma; NK/T, extranodal NK/T-cell lymphoma, nasal type.

interstitial pneumonitis.[26,27] Because most patients received TBI-based regimens as reported,[4,5,7] we failed to detect any significant differences in TRM between those who received or did not receive TBI.

Another major cause of death in our study was GVHD and/or infection. Of the 98 patients who died of treatment-related complications in our study, 29 (30%) died of infection. At least half of the patients (15 of 29) who died of infectious complications also had GVHD. In a prospective trial of allo-HSCT for patients with NHL, infection accounted for 63% of all TRM,[28] whereas other studies, including ours, have reported an incidence of 25% to 30%.[4,6] In practical transplantation procedures, complications are usually multifactorial, and it is always very difficult to define the exact cause of death, which may account for the wide variations in the incidence of infections among those who died of TRM (18%-63%) in previous reports.[4,5,28,29]

In this study, the incidence of chronic GVHD was high (48%), and chronic GVHD was a risk factor for TRM. The reason for the higher incidence of chronic GVHD in our study compared with the IBMTR report[9,30] was that the IBMTR study included data of patients who died within 100 days after allo-HSCT, whereas we excluded these patients. Unexpectedly, the incidence of chronic GVHD was higher in patients who had GVHD prophylaxis with tacrolimus plus methotrexate than in those with cyclosporin plus methotrexate. In Japan, there is a clear tendency to select tacrolimus rather than cyclosporine for GVHD prophylaxis in unrelated or HLA-mismatched transplantation.[31,32] In addition, PBSCT is not yet permitted for unrelated transplantation. Altogether, the higher incidence of GVHD observed in the tacrolimus group may simply reflect that patients with a higher risk of GVHD were selected to receive tacrolimus.

We found that the incidence of disease relapse/progression of NHL was low (21%). High TRM in the early phase of the transplantation course may mask later disease relapse/progression, and this made it difficult to estimate the relapse rate in this study. OS and PFS were not affected by the severity of acute GVHD. Our limited analysis failed to confirm a GVL effect after myeloablative allo-HSCT. Although the risk of relapse for patients with acute or chronic GVHD was not significantly different from that of patients without acute or chronic GVHD in previous studies with malignant lymphoma,[8,10,30] a study from the Japan Marrow Donor Program showed that the development of grade II to IV acute GVHD was associated with a lower incidence of disease progression after unrelated HSCT.[31] It has been reported that a low level of acute GVHD was associated with improved OS, and all levels of acute GVHD were associated with a decrease in the relapse rate for intermediate-grade NHL.[8] High levels of acute GVHD had a deleterious effect on OS but were associated with an improved relapse rate for LBL.[8] Thus, our study confirmed that greater effort is required to reduce GVHD-related complications after myeloablative allo-HSCT.

We confirmed that chemoresistance before allo-HSCT and prior autograft were significant risk factors for both OS and TRM. RIST or a less organ-toxic myeloablative allo-HSCT using a combination of fludarabine plus intravenous busulfan may be applied more safely in this population to reduce TRM.[19-21,33,34] However, further studies are needed to determine whether reduced-intensity conditioning could control activity of chemoresistant disease. In contrast to previous studies, we showed that prior radiotherapy was associated with a significantly worse OS, which may be related to the fact that 44 (54%) of the 81 patients who had a history of local radiotherapy had refractory disease at transplantation. Hence, it might be that prior radiotherapy was a marker of survival for more advanced and refractory disease.

In conclusion, we confirmed that myeloablative allo-HSCT is a curative therapeutic option in a subset of patients with NHL, but it carries a high risk of toxicities and TRM. Chemoresistant disease and a history of previous autograft are risk factors for both OS and TRM. Whether the introduction of a reduced-intensity transplantation procedure results in reduction of TRM should be evaluated, and more effective GVHD prophylaxis while maintaining a GVL effect should be developed.

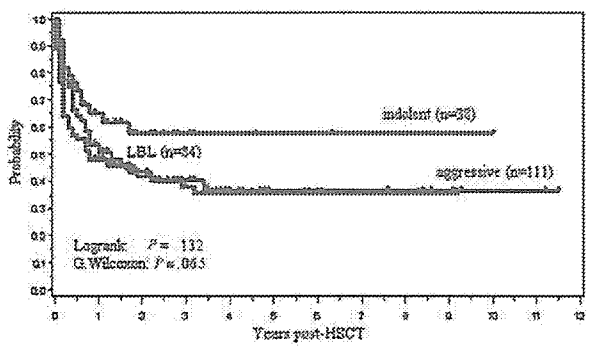

Figure 3. Overall survival stratified according to the clinical subtype. Indolent lymphoma included all grades of FL and extranodal marginal zone B-cell lymphoma of mucosa-associated lymphoid tissue. Aggressive lymphoma included all lymphomas except for indolent and lymphoblastic lymphoma (LBL).

Table 4. Univariate and multivariate analyses of overall survival

Variable	No.	Univariate analysis		Multivariate analysis	
		Hazard ratio (95% CI)	P	Hazard ratio (95% CI)	P
Age at transplant			.134	—	—
Younger than 40 y	158	1.00		—	—
40 y or older	75	1.32 (0.92-1.90)		—	—
Clinical subtype			.126	—	—
Indolent	38	1.00		—	—
Lymphoblastic	84	1.57 (0.88-2.80)		—	—
Clinical subtype			.045	—	—
Indolent	38	1.00		—	—
Aggressive	111	1.77 (1.01-3.11)		—	—
Aggressive lymphoma			.004	—	—
PTCL	22	1.00		—	—
Non-PTCL	89	3.45 (1.47-7.69)		—	—
Response to chemotherapy			< .001	—	—
Sensitive	128	1.00		—	—
Resistant	105	3.31 (2.30-4.76)		3.12 (2.16-4.51)	< .001
Prior autograft			< .001	—	—
No	193	1.00		—	—
Yes	40	2.59 (1.73-3.87)		2.18 (1.43-3.30)	< .001
Prior radiotherapy			< .001	—	—
No	152	1.00		—	—
Yes	81	1.99 (1.41-2.83)		1.47 (1.02-2.11)	.037
Years of transplantation			.932	—	—
1996-2001	187	1.00		—	—
1990-1995	46	1.02 (0.67-1.54)		—	—
Donor			.076	—	—
HLA-matched	197	1.00		—	—
HLA-mismatched	36	1.50 (0.96-2.33)		—	—
HLA-matched donor			.769	—	—
Related	154	1.00		—	—
Unrelated	43	0.93 (0.58-1.50)		—	—
Source of stem cells*			.095	—	—
BM	159	1.00		—	—
PBSCs	70	1.37 (0.95-2.00)		—	—
Conditioning regimen			.107	—	—
TBI-containing	193	1.00		—	—
Others	40	1.42 (0.93-2.17)		—	—
GVHD prophylaxis†			.227	—	—
Cyclosporin + methotrexate	204	1.00		—	—
Tacrolimus + methotrexate	22	1.40 (0.81-2.40)		—	—
Acute GVHD-time‡	—	1.25 (0.85-1.84)	.264	1.28 (0.87-1.90)	.213

CI indicates confidence interval; PTCL, peripheral T-cell lymphoma; HLA, human leukocyte antigen; BM, bone marrow; GVHD, graft-versus-host disease; and —, not applicable.

*Those who received cord blood (n = 2) or BM + PBSCs (n = 2) were excluded because of the small number of patients.

†Seven patients using other GVHD prophylaxis were excluded.

‡Acute GVHD was treated as time-dependent variable.

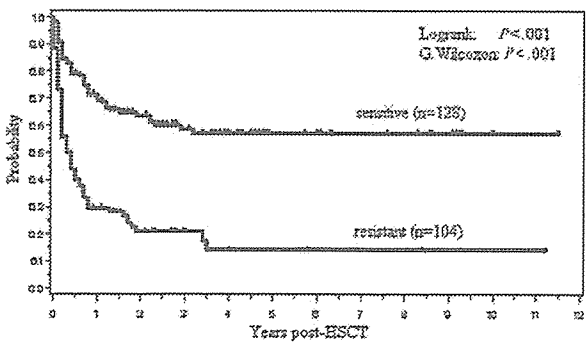

Figure 5. The relation between overall survival and response to chemotherapy.

Acknowledgments

We thank the many physicians in the participating teams who contributed to this survey.

Appendix

The following institutions contributed data to this study: Asahikawa Medical College Hospital, Hokkaido University Hospital, Sapporo Hokuyu Hospital, Akita University Hospital, Gunma Saiseikai Maebashi Hospital, Jichi Medical School Hospital, Suifu Hospital, Saitama Cancer Center Hospital, Jikei University Kashiwa Hospital, Chiba Aoba Municipal

Hospital, Tokyo Metropolitan Komagome Hospital, National Cancer Center Hospital, Keio University Hospital, Toranomon Hospital, Yokohama City University Hospital, Kanagawa Cancer Center, Tokai University Hospital, Kurobe City Hospital, Kanazawa University Hospital, Ishikawa Prefectural Central Hospital, Nagoya City University Hospital, Japanese Red Cross Nagoya First Hospital, Nagoya Daini Red Cross Hospital, Meitetsu Hospital, JA Aichi Showa Hospital, Kyoto University Hospital, Kyoto Prefectural University of Medicine Hospital, Osaka University Hospital, Osaka City University Hospital, Kansai Medical University Hospital, Kinki University Hospital, Osaka Medical Center for Cancer and Cardiovascular Diseases, Osaka City General Hospital, Rinku General Medical Center Izumisano Hospital, Hyogo College of Medicine Hospital, Hyogo Medical Center for Adults, Okayama University Hospital, Okayama Medical Center, Shimane Prefectural Central Hospital, Takamatsu Red Cross Hospital, Ehime Prefectural Central Hospital, University of Occupational and Environmental Health Hospital, Kitakyushu Municipal Medical Center, Kyushu Cancer Center, Kokura Memorial Hospital, Fukuoka University Hospital, Hamanomachi Hospital, Harasanshin Hospital, Saga Prefectural Hospital Koseikan, Sasebo Municipal General Hospital, Miyazaki Prefectural Miyazaki Hospital, Imamura Bun-in Hospital, and Ryukyu University Hospital.

References

1. Philip T, Guglielmi C, Hagenbeek A, et al. Autologous bone marrow transplantation as compared with salvage chemotherapy in relapses of chemotherapy-sensitive non-Hodgkin's lymphoma. N Engl J Med. 1995;333:1540-1545.
2. Milpied N, Deconinck E, Gaillard F, et al. Initial treatment of aggressive lymphoma with high-dose chemotherapy and autologous stem-cell support. N Engl J Med. 2004;350:1287-1295.
3. Horning SJ, Negrin RS, Hoppe RT, et al. High-dose therapy and autologous bone marrow transplantation for follicular lymphoma in first complete or partial remission: results of a phase II clinical trial. Blood. 2001;97:404-409.
4. Dhedin N, Giraudier S, Gaulard P, et al. Allogeneic bone marrow transplantation in aggressive non-Hodgkin's lymphoma (excluding Burkitt and lymphoblastic lymphoma): a series of 73 patients from the SFGM database. Br J Haematol. 1999; 107:154-161.
5. van Besien KW, Mehra RC, Giralt SA, et al. Allogeneic bone marrow transplantation for poor-prognosis lymphoma: response, toxicity and survival depend on disease histology. Am J Med. 1996;100:299-307.
6. van Besien K, Thall P, Korbling M, et al. Allogeneic transplantation for recurrent or refractory non-Hodgkin's lymphoma with poor prognostic features after conditioning with thiotepa, busulfan, and cyclophosphamide: experience in 44 consecutive patients. Biol Blood Marrow Transplant. 1997;3:150-156.
7. van Besien K, Sobocinski KA, Rowlings PA, et al. Allogeneic bone marrow transplantation for low-grade lymphoma. Blood. 1998;92:1832-1836.
8. Peniket AJ, Ruiz de Elvira MC, Taghipour G, et al. An EBMT registry matched study of allogeneic stem cell transplants for lymphoma: allogeneic transplantation is associated with a lower relapse rate but a higher procedure-related mortality rate than autologous transplantation. Bone Marrow Transplant. 2003;31:667-678.
9. Levine JE, Harris RE, Loberiza FR Jr, et al. A comparison of allogeneic and autologous bone marrow transplantation for lymphoblastic lymphoma. Blood. 2003;101:2476-2482.
10. van Besien K, Loberiza FR Jr, Bajorunaite R, et al. Comparison of autologous and allogeneic hematopoietic stem cell transplantation for follicular lymphoma. Blood. 2003;102:3521-3529.
11. Forrest DL, Thompson K, Nevill TJ, Couban S, Fernandez LA. Allogeneic hematopoietic stem cell transplantation for progressive follicular lymphoma. Bone Marrow Transplant. 2002;29:973-978.
12. Berdeja JG, Jones RJ, Zahurak ML, et al. Allogeneic bone marrow transplantation in patients with sensitive low-grade lymphoma or mantle cell lymphoma. Biol Blood Marrow Transplant. 2001;7: 561-567.
13. Stein RS, Greer JP, Goodman S, et al. Limited efficacy of intensified preparative regimens and autologous transplantation as salvage therapy in high-grade non-Hodgkin's lymphoma. Leuk Lymphoma. 2001;40:521-528.
14. Khouri IF, Lee MS, Romaguera J, et al. Allogeneic hematopoietic transplantation for mantle-cell lymphoma: molecular remissions and evidence of graft-versus-malignancy. Ann Oncol. 1999;10: 1293-1299.
15. Zaja F, Russo D, Silvestri F, et al. Retrospective analysis of 23 cases with peripheral T-cell lymphoma, unspecified: clinical characteristics and outcome. Haematologica. 1997;82:171-177.
16. Makita M, Maeda Y, Takenaka K, et al. Successful treatment of progressive NK cell lymphoma with allogeneic peripheral stem cell transplantation followed by early cyclosporine tapering and donor leukocyte infusions. Int J Hematol. 2002;76:94-97.
17. Khouri IF, Lee MS, Saliba RM, et al. Nonablative allogeneic stem-cell transplantation for advanced/recurrent mantle-cell lymphoma. J Clin Oncol. 2003;21:4407-4412.
18. Khouri IF, Saliba RM, Giralt SA, et al. Nonablative allogeneic hematopoietic transplantation as adoptive immunotherapy for indolent lymphoma: low incidence of toxicity, acute graft-versus-host disease, and treatment-related mortality. Blood. 2001;98:3595-3599.
19. Tanimoto TE, Kusumi E, Hamaki T, et al. High complete response rate after allogeneic hematopoietic stem cell transplantation with reduced-intensity conditioning regimens in advanced malignant lymphoma. Bone Marrow Transplant. 2003;32:131-137.
20. Bierman PJ. Allogeneic bone marrow transplantation for lymphoma. Blood Rev. 2000;14:1-13.
21. Jaffe ES, Harris NL, Stein H, et al, eds. World Health Organization Classification of Tumors. Pathology and Genetics of Tumours of Haematopoietic and Lymphoid Tissues. Lyon, France: IARC Press; 2001.
22. Przepiorka D, Weisdorf D, Martin P, et al. 1994 Consensus Conference on Acute GVHD Grading. Bone Marrow Transplant. 1995;15:825-828.
23. Shulman HM, Sullivan KM, Weiden PL, et al. Chronic graft-versus-host syndrome in man. A long-term clinicopathologic study of 20 Seattle patients. Am J Med. 1980;69:204-217.
24. Kaplan EL, Meier P. Nonparametric estimation from incomplete observations. Am Stat Assoc J. 1958;457-481.
25. Akpek G, Ambinder RF, Piantadosi S, et al. Long-term results of blood and marrow transplantation for Hodgkin's lymphoma. J Clin Oncol. 2001;19: 4314-4321.
26. Bortin MM, Kay HE, Gale RP, Rimm AA. Factors associated with interstitial pneumonitis after bone-marrow transplantation for acute leukaemia. Lancet. 1982;1:437-439.
27. Weiner RS, Bortin MM, Gale RP, et al. Interstitial pneumonitis after bone marrow transplantation. Assessment of risk factors. Ann Intern Med. 1986;104:168-175.
28. Ratanatharathorn V, Uberti J, Karanes C, et al. Prospective comparative trial of autologous versus allogeneic bone marrow transplantation in patients with non-Hodgkin's lymphoma. Blood. 1994;84:1050-1055.
29. Chopra R, Goldstone AH, Pearce R, et al. Autologous versus allogeneic bone marrow transplantation for non-Hodgkin's lymphoma: a case-controlled analysis of the European Bone Marrow Transplant Group Registry data. J Clin Oncol. 1992;10:1690-1695.
30. Freytes CO, Loberiza FR, Rizzo JD, et al. Myeloablative allogeneic hematopoietic stem cell transplantation in patients who experience relapse after autologous stem cell transplantation for lymphoma: a report of the International Bone Marrow Transplant Registry. Blood. 2004;104: 3797-3803.
31. Izutsu K, Kanda Y, Ohno H, et al. Unrelated bone marrow transplantation for non-Hodgkin lymphoma: a study from the Japan Marrow Donor Program. Blood. 2004;103:1955-1960.
32. Yanada M, Emi N, Naoe T, et al. Tacrolimus instead of cyclosporine used for prophylaxis against graft-versus-host disease improves outcome after hematopoietic stem cell transplantation from unrelated donors, but not from HLA-identical sibling donors: a nationwide survey conducted in Japan. Bone Marrow Transplant. 2004;34:331-337.
33. de Lima M, Couriel D, Thall PF, et al. Once-daily intravenous busulfan and fludarabine: clinical and pharmacokinetic results of a myeloablative, reduced-toxicity conditioning regimen for allogeneic stem cell transplantation in AML and MDS. Blood. 2004;104:857-864.
34. Russell JA, Tran HT, Quinlan D, et al. Once-daily intravenous busulfan given with fludarabine as conditioning for allogeneic stem cell transplantation: study of pharmacokinetics and early clinical outcomes. Biol Blood Marrow Transplant. 2002;8: 468-476.

Development of functional human blood and immune systems in NOD/SCID/IL2 receptor γ chain^{null} mice

Fumihiko Ishikawa, Masaki Yasukawa, Bonnie Lyons, Shuro Yoshida, Toshihiro Miyamoto, Goichi Yoshimoto, Takeshi Watanabe, Koichi Akashi, Leonard D. Shultz, and Mine Harada

Here we report that a new nonobese diabetic/severe combined immunodeficient (NOD/SCID) mouse line harboring a complete null mutation of the common cytokine receptor γ chain (NOD/SCID/interleukin 2 receptor [IL2r] γ^{null}) efficiently supports development of functional human hemato-lymphopoiesis. Purified human (h) CD34$^+$ or hCD34$^+$hCD38$^-$ cord blood (CB) cells were transplanted into NOD/SCID/IL2rγ^{null} newborns via a facial vein. In all recipients injected with 10^5 hCD34$^+$ or 2×10^4 hCD34$^+$hCD38$^-$ CB cells, human hematopoietic cells were reconstituted at approximately 70% of chimerisms. A high percentage of the human hematopoietic cell chimerism persisted for more than 24 weeks after transplantation, and hCD34$^+$ bone marrow grafts of primary recipients could reconstitute hematopoiesis in secondary NOD/SCID/IL2rγ^{null} recipients, suggesting that this system can support self-renewal of human hematopoietic stem cells. hCD34$^+$hCD38$^-$ CB cells differentiated into mature blood cells, including myelomonocytes, dendritic cells, erythrocytes, platelets, and lymphocytes. Differentiation into each lineage occurred via developmental intermediates such as common lymphoid progenitors and common myeloid progenitors, recapitulating the steady-state human hematopoiesis. B cells underwent normal class switching, and produced antigen-specific immunoglobulins (Igs). T cells displayed the human leukocyte antigen (HLA)–dependent cytotoxic function. Furthermore, human IgA-secreting B cells were found in the intestinal mucosa, suggesting reconstitution of human mucosal immunity. Thus, the NOD/SCID/IL2rγ^{null} newborn system might be an important experimental model to study the human hemato-lymphoid system. (Blood. 2005;106:1565-1573)

Introduction

To analyze human immune and hematopoietic development and function in vivo, a number of studies have been tried to reproduce human hematopoiesis in small animal xenotransplantation models.[1] Successful transplantation of human hematopoietic tissues in immune-compromised mice was first reported in late 1980s by using homozygous severe combined immunodeficient (C.B.17-SCID) mice. In the first model of a humanized lymphoid system in a SCID mouse (SCID-hu model), McCune et al simultaneously transplanted human fetal tissues, including fetal liver hematopoietic cells, thymus, and lymph nodes, into SCID mice and induced mature human T- and B-cell development.[2] Mosier et al successfully reconstituted human T and B cells by transferring human blood mononuclear cells into SCID mice.[3] These initial studies suggested the usefulness of immunodeficient mice for reconstitution of the human lymphoid system from human bone marrow hematopoietic stem cells (HSCs).

After these initial reports, a number of modified SCID models have been proposed to try to reconstitute human immunity.[4] In addition, recombination activating gene (RAG)–deficient strains have been used as recipients in xenotransplantation: T- and B-cell–deficient *Prkdc*^{scid}, *Rag1*$^{-/-}$, or *Rag2*$^{-/-}$ mutant mice[5-7] were capable of supporting engraftment of human cells. The engraftment levels in these models, however, were still low, presumably due to the remaining innate immunity of host animals.[1] Nonobese diabetic/severe combined immunodeficient (NOD/SCID) mice have been shown to support higher levels of human progenitor cell engraftment than BALB/c/SCID or C.B.17/SCID mice.[8] Levels of human cell engraftment were further improved by treating NOD/SCID mice with anti-asialo GM1 (ganglioside-monosialic acid) antibodies[9] that can abrogate natural killer (NK) cell activity. Recently, NOD/SCID mice harboring either a null allele at the β_2-microglobulin gene (NOD/SCID/β2m$^{-/-}$)[10] or a truncated common cytokine receptor γ chain (γc) mutant lacking its cytoplasmic region (NOD/SCID/γ$_c^{-/-}$)[11,12] were developed. In these mice, NK- as well as T- and B-cell development and functions are disrupted, because β2m is necessary for major histocompatibility complex (MHC) class I–mediated innate immunity, and because γc (originally called IL-2Rγ chain) is an indispensable component

From the Department of Medicine and Biosystemic Science, Kyushu University Graduate School of Medical Sciences, Fukuoka, Japan; First Department of Internal Medicine, Ehime University School of Medicine, Shigenobu, Japan; The Jackson Laboratory, Bar Harbor, ME; Center for Cellular and Molecular Medicine, Kyushu University Hospital, Fukuoka, Japan; RIKEN for Allergy and Immunology, Yokohama, Japan; and the Department of Cancer Immunology and AIDS, Dana-Farber Cancer Institute, Boston, MA.

Submitted February 9, 2005; accepted April 7, 2005. Prepublished online as *Blood* First Edition Paper, May 26, 2005; DOI 10.1182/blood-2005-02-0516.

Supported by grants from Japan Society for Promotion of Science (F.I.); the Ministry of Education, Culture, Sports, Science and Technology of Japan (M.Y.); the Ministry of Health, Labor, and Welfare of Japan (M.H.); and National Institutes of Health grants A130389 and HL077642 (L.D.S.) and DK061320 (K.A.).

The online version of the article contains a data supplement.

Reprints: Koichi Akashi, Department of Cancer Immunology and AIDS, Dana-Farber Cancer Institute, 44 Binney St, no. 770, Boston, MA 02115; e-mail: koichi_akashi@dfci.harvard.edu; or Leonard D. Shultz, The Jackson Laboratory, 600 Main St, Bar Harbor, ME 04609.

The publication costs of this article were defrayed in part by page charge payment. Therefore, and solely to indicate this fact, this article is hereby marked "advertisement" in accordance with 18 U.S.C. section 1734.

of receptor heterodimers for many lymphoid-related cytokines (ie, IL-2, IL-7, IL-9, IL-12, IL-15, and IL-21).[13] Injection of human bone marrow or cord blood (CB) cells into these mice resulted in successful generation of human T and B cells. In our hands, efficiencies of CB cell engraftment represented by percentages of circulating human (h) CD45$^+$ cells were significantly (2- to 5-fold) higher in NOD/SCID/β2m$^{-/-}$ newborns than those in adults (F.I., M.H., and L.D.S., unpublished data, April 2003). More recently, transplantation of hCD34$^+$ CB cells into Rag2$^{-/-}$ γc$^{-/-}$ newborns regenerated adaptive immunity mediated by functional T and B cells,[14] suggesting heightened support for xenogeneic transplants especially in the neonatal period. Efficiency of reconstitution of human hematopoiesis may be, however, still suboptimal in these models because chimerisms of human cells are not stable in each experiment.[11,12,14] Furthermore, there is little information regarding reconstitution of human myeloerythroid components in these xenogeneic models.

Two types of mouse lines with truncated or complete null γc mutant[15-17] have been reported. NOD/SCID/$\gamma_c^{-/-}$ and Rag2$^{-/-}$ γc$^{-/-}$ mouse strains harbor a truncated γc mutant lacking the intracellular domain,[15] and therefore, binding of γc-related cytokines to each receptor should normally occur in these models.[18] For example, IL-2R with the null γc mutations would be an $\alpha\beta$ heterodimer complex with an affinity approximately 10 times lower than that of the high affinity $\alpha\beta\gamma$ heterotrimer complex in mice with the truncated γc mutant.[19] γc has also been shown to dramatically increase the affinity to its ligands through the receptors for IL-4, IL-7, and IL-15.[20-23] Previous studies suggested that γc-related receptors including IL-2Rβ chain and IL-4Rα chain could activate janus-activated kinases (JAKs) to some extent in the presence of the extracellular domain of γc, independent of the cytoplasmic domain of γc.[24,25] Thus, in order to block the signaling through γc-related cytokine receptors more completely, we made NOD/SCID mice harboring complete null mutation of γc[16] (the NOD/SCID/IL2rγ^{null} strain). By using NOD/SCID/IL2rγ^{null} newborns, we successfully reconstituted myeloerythroid as well as lymphoid maturation by injecting human CB or highly-enriched CB HSCs at a high efficiency. Reconstitution of human hematopoiesis persisted for a long term. The developing lymphoid cells were functional for immunoglobulin (Ig) production and human leukocyte antigen (HLA)–dependent cytotoxic activity. Our data show that the NOD/SCID/IL2rγ^{null} newborn system provides a valuable tool to reproduce human hemato-lymphoid development.

Materials and methods

Mice

NOD.Cg-*Prkdc*^{scid}*IL2rg*^{tmlWjl}/Sz (NOD/SCID/IL2rγ^{null}) and NOD/LtSz-*Prkdc*^{scid}*/B2m*^{null} (NOD/SCID/β2m^{null}) mice were developed at the Jackson Laboratory (Bar Harbor, ME). The NOD/SCID/IL2rγ^{null} strain was established by backcrossing a complete null mutation at γc locus[16] onto the NOD.Cg-*Prkdc*^{scid} strain. The establishment of this mouse line has been reported elsewhere.[26] All experiments were performed according to the guideline in the Institutional Animal Committee of Kyushu University.

Cell preparation and transplantation

CB cells were obtained from Fukuoka Red Cross Blood Center (Japan). CB cells were harvested after written informed consent. Mononuclear cells were depleted of Lin$^+$ cells using mouse anti-hCD3, anti-hCD4, anti-hCD8, anti-hCD11b, anti-hCD19, anti-hCD20, anti-hCD56, and anti–human glycophorin A (hGPA) monoclonal antibodies (BD Immunocytometry, San Jose, CA). Samples were enriched for hCD34$^+$ cells by using anti-hCD34 microbeads (Miltenyi Biotec, Auburn, CA). These cells were further stained with anti-hCD34 and hCD38 antibodies (BD Immunocytometry), and were purified for Lin$^-$CD34$^+$CD38$^-$ HSCs by a FACSVantage (Becton Dickinson, San Jose, CA). Lin$^-$ hCD34$^+$ cells (10^5) or 2×10^4 Lin$^-$hCD34$^+$hCD38$^-$ cells were transplanted into irradiated (100 cGy) NOD/SCID/IL2rγ^{null} or NOD/SCID/β2m^{null} newborns via a facial vein[27] within 48 hours of birth.

Examination of hematopoietic chimerism

At 3 months after transplantation, samples of peripheral blood, bone marrow, spleen, and thymus were harvested from recipient mice. Human common lymphoid progenitors were analyzed based on the expression of hCD127 (IL-7 receptor α chain) and hCD10 in Lin (hCD3, hCD4, hCD8, hCD11b, hCD19, hCD20, hCD56, and hGPA)$^-$ hCD34$^+$hCD38$^+$ fraction.[28,29] Human myeloid progenitors were analyzed based on the expressions of hCD45RA and hCD123 (IL-3 receptor α chain) in Lin$^-$ CD10$^-$CD34$^+$CD38$^+$ fractions. For the analysis of megakaryocyte/erythroid (MegE) lineages, anti-hCD41a (HIP8), anti-hGPA (GAR-2), anti-mCD41a (MW Reg30), and anti-mTer119 (Ter-119) antibodies were used. Samples were treated with ammonium chloride to eliminate mature erythrocytes, and were analyzed by setting nucleated cell scatter gates. For the analysis of circulating erythrocytes and platelets, untreated blood samples were analyzed by setting scatter gates specific for each cell fraction. Human B lymphoid progenitors were evaluated according to the criteria proposed by LeBien.[30]

Methylcellulose culture assay

Bone marrow cells of recipient mice were stained with anti-hCD34, hCD38, hCD45RO, hCD123, and lineage antibodies. Human HSCs, CMPs, GMPs, and MEPs were purified according to the phenotypic definition[28,29] by using a FACSVantage (Becton Dickinson). One hundred cells of each population were cultured in methylcellulose media (Stem Cell Technologies, Vancouver, BC, Canada) supplemented with 10% bovine serum albumin (BSA), 20 μg/mL steel factor, 20 ng/mL IL-3, 20 ng/mL IL-11, 20 ng/mL Fms-like tyrosine kinase 3 (Flt3) ligand, 50 ng/mL granulocyte-macrophage colony-stimulating factor (GM-CSF), 4 U/ml erythropoietin (Epo), and 50 ng/mL thrombopoietin (Tpo). Colony numbers were enumerated on day 14 of culture.

Histologic analysis

Tissue samples were fixed with 4% paraformaldehyde and dehydrated with graded alcohol. After treatment with heated citrate buffer for antigen retrieval, paraformaldehyde-fixed paraffin-embedded sections were immunostained with mouse anti-hCD19, anti–human IgA, anti-hCD3, anti-hCD4, anti-hCD8, and anti-hCD11c antibodies (Dako Cytomation, Carpinteria, CA). Stained specimens were observed by confocal microscopy (LSM510 META microscope; Carl Zeiss, Oberkochen, Germany). Image acquisition and data analysis were performed by using LSM5 software. Numerical aperture of the objective lens (PlanApochromat ×63) used was 1.4.

ELISA

Human Ig concentration in recipient sera was measured by using a human immunoglobulin assay kit (Bethyl, Montgomery, IL). For detection of ovalbumin (OVA)–specific human IgM and IgG antibodies, 5 recipient mice were immunized twice every 2 weeks with 100 μg of OVA (Sigma, St Louis, MO) that were emulsified in aluminum hydroxide (Sigma). Sera from OVA-treated mice were harvested 2 weeks after the second immunization. OVA was plated at s concentration of 20 μg/mL on 96-microtiter wells at 4°C overnight. After washing and blocking with bovine serum albumin, serum samples were incubated in the plate for 1 hour. Antibodies binding OVA were then measured by a standard enzyme-linked immunosorbent assay (ELISA).

Cytotoxicity of alloantigen-specific human CD4+ and CD8+ T-cell lines

Alloantigen-specific human CD4+ and CD8+ T-cell lines were established according to the method as reported.[31] After stimulation with an Epstein Barr virus–transformed B lymphoblastoid cell line (TAK-LCL) established from a healthy individual (TAK-LCL) for 6 days, 100 hCD4+ T cells or hCD8+ T cells were plated with 3×10^4 TAK-LCL cells in the presence of 10 U/mL human IL-2 (Genzyme, Boston, MA), and were subjected to a chromium 51 (^{51}Cr) release assay. A Limiting number of effector cells and 10^4 ^{51}Cr-labeled allogeneic target cells were incubated. KIN-LCLs that do not share HLA with effector cells or TAK-LCL were used as negative controls. Cytotoxic activity was tested in the presence or absence of anti-HLA class I or anti–HLA-DR monoclonal antibodies.

Results

Reconstitution of human hematopoiesis is achieved in NOD/SCID/IL2rγ^{null} mice

NOD/SCID/IL2rγ^{null} mice lacked mature murine T or B cells evaluated by fluorescence-activated cell sorting (FACS), and displayed extremely low levels of NK cell activity.[31] This mouse line can survive more than 15 months[31] since it does not develop thymic lymphoma, usually a fatal disease in the immune-compromised mice with NOD background.[32]

Lin−hCD34+ CB cells contain HSCs, and myeloid and lymphoid progenitors.[28,29] We and others have reported that engraftment of human CB cells, which contain hematopoietic stem and progenitor cells, was efficient in NOD/SCID/β2m$^{-/-}$ and RAG2$^{-/-}$/γ$_c^{-/-}$ mice, especially when cells were transplanted during the neonatal period.[14,33] We therefore transplanted purified Lin−hCD34+ CB cells into sublethally irradiated NOD/SCID/IL2rγ^{null} newborns via a facial vein.[27]

We first transplanted 10^5 Lin−hCD34+ CB cells from 3 independent donors into 5 NOD/SCID/IL2rγ^{null} newborns, and found that the NOD/SCID/IL2rγ^{null} newborn system is very efficient for supporting engraftment of human hematopoietic progenitor cells. Table 1 shows percentages of hCD45+ cells in these mice 3 months after transplantation. Strikingly, the average engraftment levels were approximately 70% in both the bone marrow and the peripheral blood. Compared with 4 control NOD/SCID/β2m$^{-/-}$ recipient mice given transplants from the same donors, engraftment levels of hCD45+ cells in NOD/SCID/IL2rγ^{null} mice were significantly higher (Table 1).

Table 1. Chimerism of human CD45+ cells in NOD/SCID/β2m^{null} mice and NOD/SCID/IL2rγ^{null} mice

Mouse no. (donor no.)	% nucleated cells		
	PB	BM	Spleen
NOD/SCID/IL2rγ^{null}			
1 (1)	71.2	70.9	66.8
2 (1)	81.7	81.4	47.1
3 (2)	50.1	58.8	49.5
4 (3)	68.0	83.1	51.1
5 (3)	73.3	70.1	58.1
Mean ± SD	68.9 ± 11.6*	72.9 ± 9.8*	54.5 ± 8.0*
NOD/SCID/β2m^{null}			
1 (1)	10.4	46.1	22.0
2 (2)	11.6	31.5	24.3
3 (3)	6.9	18.1	20.7
4 (3)	20.7	30.4	31.2
Mean ± SD	12.4 ± 5.9*	31.5 ± 11.5*	22.6 ± 4.7*

To compare the engraftment levels in the two strains, 1×10^5 Lin− CD34+ cells derived from 3 CB samples were transplanted into 5 NOD/SCID/IL2rγ^{null} mice and 4 NOD/SCID/β2m^{null} mice. At 3 months after transplantation, BM, spleen, and peripheral blood (PB) of the recipient mice were analyzed for the engraftment of human cells. Data show percentages of human CD45+ cells in each tissue.

*$P < .05$.

Table 2 shows the analysis of human hematopoietic cell progeny in mice that received transplants of human Lin−hCD34+ CB cells. In the peripheral blood, hCD45+ cells included hCD33+ myeloid, hCD19+ B cells, and hCD3+ T cells in all mice analyzed (Figure 1A and Table 2). We then analyzed the reconstitution of erythropoiesis and thrombopoiesis in these mice. Anti–human glycophorin A (hGPA) antibodies recognized human erythrocytes, while mTer119 antibodies[34] recognized GPA-associated protein on murine erythrocytes, respectively (Figure 1B). Human and murine platelets could also be stained with anti–human and anti–murine CD41a, respectively (Figure 1B). Circulating hGPA+ erythrocytes and hCD41a+ platelets were detected in all 3 mice analyzed (Figure 1B, right panels). hGPA+ erythroblasts and hCD41a+ megakaryocytes were detected as 9.5% ± 6.2% (n = 5) and 1.64% ± 0.42% (n = 5) of nucleated bone marrow cells, respectively. Thus, transplanted human Lin−hCD34+ CB cells differentiated into mature erythrocytes and platelets in NOD/SCID/IL2rγ^{null} recipients.

In all engrafted mice, the bone marrow and the spleen contained significant numbers of hCD11c+ dendritic cells as well as hCD33+ myeloid cells, hCD19+ B cells, and hCD3+ T cells (Table 2 and Figure 1C). hCD11c+ dendritic cells coexpressed HLA-DR that is essential for antigen presentation to T cells (Figure 1D). In contrast, in the thymus, the majority of cells were composed of hCD3+ T cells and rare hCD19+ B cells (Table 2).

Figure 2A shows the change in the percentage of circulating hCD45+ cells in another set of NOD/SCID/IL2rγ^{null} newborns injected with 2×10^4 Lin−hCD34+hCD38− CB cells. Surprisingly, the level of hCD45+ cells in the blood was unchanged, and was maintained at a high level even 24 weeks after transplantation. Mice did not develop lymphoid malignancies or other complications. Furthermore, we tested the retransplantability of human HSCs in primary recipients. We killed mice at 24 weeks after the primary transplantation of hCD34+ cells, purified 1 to 5×10^4 hCD34+ cells from primary recipient bone marrow cells, and retransplanted them into NOD/SCID/IL2rγ^{null} newborns. In all 3 experiments, secondary recipients successfully reconstituted human hematopoiesis at least until 12 weeks after transplantation, when we killed mice for the bone marrow analysis (Figure 2B). Thus, the NOD/SCID/IL2rγ^{null} newborn system can support human hematopoiesis for the long term.

Human cord blood hematopoietic stem cells produced myeloid and lymphoid cells via developmental intermediates in the NOD/SCID/IL2rγ^{null} bone marrow

The Lin−hCD34+ CB fraction contains early myeloid and lymphoid progenitors as well as HSCs.[28] To verify that differentiation into all hematopoietic cells can be initiated from human HSCs in the NOD/SCID/IL2rγ^{null} newborn system, we transplanted Lin−hCD34+hCD38− CB cells that contain the counterpart population of murine long-term HSCs,[35] and are highly enriched for human HSCs.[36,37] hCD34+ CB cells (15%-20%) were hCD38− (data not shown). Mice given transplants of 2×10^4 Lin−hCD34+hCD38− cells displayed successful reconstitution of similar proportion of human cells compared with mice reconstituted with 1×10^5 Lin−hCD34+ cells at 12 weeks after transplantation (Table 2). In another experiment, mice injected with 2×10^4 Lin−hCD34+hCD38− cells exhibited the high chimerism (> 50%)

Table 2. Cellular number and composition in tissues of engrafted NOD/SCID/IL2rγ^{null} mice

Injected cells, mice, and tissue type	Total no. cells	% nucleated cells (% hCD45$^+$ cells)			
		CD33	CD19	CD3	CD11c
1 × 10^5 Lin$^-$CD34$^+$					
Mouse no. 1/ donor no. 1					
BM	2.4 × 10^7	8.2 (11.6)	54.8 (77.6)	10.7 (15.1)	1.1 (1.6)
Spleen	4.1 × 10^7	4.3 (6.4)	33.5 (50.1)	26.1 (39.1)	2.2 (3.3)
Thymus	3.1 × 10^5	NE	1.3 (1.3)	96.2 (98.7)	NE
PB	NE	4.0 (5.6)	35.1 (49.3)	19.8 (27.8)	NE
Mouse no. 2/donor no. 1					
BM	1.8 × 10^7	5.5 (6.8)	56.5 (67.6)	9.9 (12.2)	2.9 (3.6)
Spleen	3.2 × 10^7	2.1 (4.5)	27.7 (58.8)	15.9 (33.8)	1.3 (2.8)
Thymus	4.5 × 10^5	NE	1.1 (1.2)	90.4 (98.8)	NE
PB	NE	6.1 (7.5)	53.8 (65.9)	21.6 (40.1)	NE
Mouse no. 4/ donor no. 3					
BM	1.9 × 10^7	9.4 (11.3)	52.9 (63.7)	15.9 (19.1)	0.62 (0.75)
Spleen	4.4 × 10^7	3.5 (6.8)	24.2 (47.4)	20.8 (40.7)	1.5 (2.9)
Thymus	0.8 × 10^5	NE	0.88 (1.1)	78.2 (98.9)	NE
PB	NE	3.2 (4.7)	61.3 (90.1)	5.3 (7.8)	NE
Mouse no. 5/donor no. 3					
BM	2.1 × 10^7	10.2 (14.6)	48.8 (82.0)	9.4 (13.4)	1.3 (1.9)
Spleen	2.7 × 10^7	6.6 (11.4)	30.4 (52.3)	18.6 (32.0)	1.1 (1.9)
Thymus	1.1 × 10^5	NE	3.1 (3.7)	81.1 (96.3)	NE
PB	NE	9.8 (13.4)	40.4 (55.1)	16.8 (22.9)	NE
2 × 10^4 Lin$^-$CD34$^+$CD38$^-$					
Mouse no. 6/donor no. 4					
BM	2.6 × 10^7	3.1 (5.3)	46.1 (78.7)	8.1 (13.8)	1.3 (2.2)
Spleen	3.9v10^7	1.3 (2.7)	40.2 (83.9)	5.9 (12.3)	0.54 (1.1)
Thymus	1.9 × 10^5	NE	2.1 (2.3)	89.4 (97.7)	NE
PB	NE	5.4 (12.4)	28.9 (66.3)	9.3 (21.3)	NE
Mouse no. 7/donor no. 5					
BM	1.4 × 10^7	7.2 (14.2)	39.6 (78.1)	3.1 (6.1)	0.82 (1.6)
Spleen	2.2 × 10^7	2.4 (5.1)	37.2 (79.3)	6.8 (14.5)	0.52 (1.1)
Thymus	1.3 × 10^5	NE	0.6 (0.7)	85.1 (99.2)	NE
PB	NE	2.3 (41.7)	49.3 (89.5)	3.5 (6.4)	NE
Mouse no. 8/donor no. 6					
BM	1.1 × 10^7	6.1 (11.7)	36.8 (70.6)	7.7 (14.8)	2.5 (4.8)
Spleen	2.9 × 10^7	2.9 (4.6)	33.8 (53.1)	24.6 (38.6)	2.4 (3.8)
Thymus	1.9 × 10^5	NE	1.1 (1.2)	94.1 (97.0)	NE
PB	NE	8.1 (11.9)	50.2 (73.5)	10.0 (14.6)	NE

BM, spleen, and thymus were harvested from engrafted NOD/SCID/IL2rγ^{null} mice at 3 months after transplantation. Total cell numbers in BM and thymus represent the cells harvested from 2 femurs for BM and those harvested from a hemilobe for thymus. Recipients 1, 2, 4, and 5 received transplants of 1 × 10^5 Lin$^-$CD34$^+$ cells. Recipients 6, 7, and 8 received transplants of 2 × 10^4 Lin$^-$CD34$^+$CD38$^-$ cells. NE indicates not examined.

of circulating human blood cells even 24 weeks after transplantation (not shown), suggesting the long-term engraftment of self-renewing human HSCs.

In all mice injected with Lin$^-$hCD34$^+$hCD38$^-$ cells, hGPA$^+$ erythroid cells and hCD41a$^+$ megakaryocytes were present (not shown). We then tested whether differentiation of Lin$^-$hCD34$^+$hCD38$^-$ HSCs in the NOD/SCID/IL2rγ^{null} mouse microenvironment can recapitulate normal developmental processes in the human bone marrow. We and others have reported that phenotypically separable myeloid and lymphoid progenitors are present in the steady-state normal bone marrow in both mice[38,39] and humans.[28,29] Figure 2C shows the representative FACS analysis data of recipient's bone marrow cells. In all 3 mice tested, the bone marrow contained the hCD34$^+$hCD38$^-$ HSC[36,37] and the hCD34$^+$hCD38$^+$ progenitor fractions.[28] The hCD34$^+$hCD38$^+$hCD10$^+$hCD127 (IL-7Rα)$^+$ common lymphoid progenitor (CLP) population[29] was detected (Figure 2C, top panels). According to the phenotypic definition of human myeloid progenitors,[28] the hCD34$^+$hCD38$^+$ progenitor fraction was subfractionated into hCD45RA$^-$hCD123 (IL-3Rα)^{lo} common myeloid progenitor (CMP), hCD45RA$^-$hCD123$^-$ megakaryocyte/erythrocyte progenitor (MEP), and hCD45RA$^+$hCD123^{lo} granulocyte/monocyte progenitor (GMP) populations (Figure 2C, bottom panels). We then purified these myeloid progenitors, and tested their differentiation potential. As shown in Figure 2D, purified GMPs and MEPs generated granulocyte/monocyte (GM)– and megakaryocyte/erythrocyte (MegE)–related colonies, respectively, while CMPs as well as HSCs generated mixed colonies in addition to GM and MegE colonies. These data strongly suggest that hCD34$^+$hCD38$^-$ human HSCs differentiate into all myeloid and lymphoid lineages tracking normal developmental steps of the steady-state human hematopoiesis within the NOD/SCID/IL2rγ^{null} mouse bone marrow.

Development of human systemic and mucosal immune systems in NOD/SCID/IL2rγ^{null} mice

We further evaluated development of the human immune system in NOD/SCID/IL2rγ^{null} recipients. In the thymus, thymocytes were mostly consisted of hCD3$^+$ T cells with scattered hCD19$^+$ B cells (Figure 3A-B). This is reasonable since the normal murine thymus contain a small number of B cells in addition to T cells.[40]

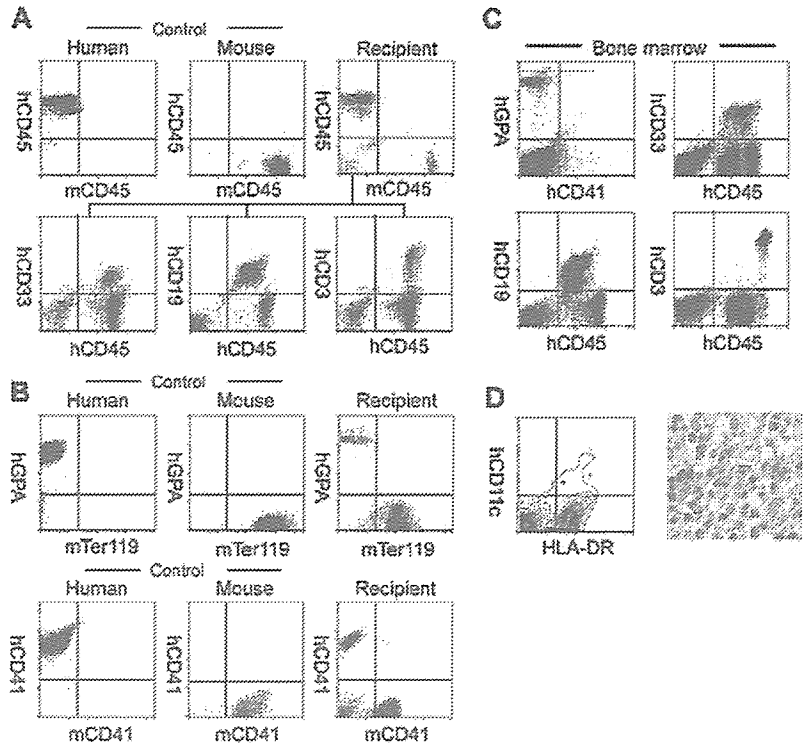

Figure 1. Analysis of human hematopoietic cells in NOD/SCID/IL2rγ^{null} recipients. (A) In the scatter gates for nucleated cells, anti-hCD45 and anti-mCD45 antibodies (Abs) reacted exclusively with human and murine leukocytes, respectively. In the recipient blood, the majority of nucleated cells were human leukocytes (top row). High levels of engraftment by hCD33$^+$ myelomonocytic cells, hCD19$^+$ B cells, and hCD3$^+$ T cells were achieved in peripheral blood of recipient mice given transplants of Lin$^-$hCD34$^+$ CB cells (bottom row). (B) Analysis of circulating erythrocytes (top row) or platelets (bottom row) in a NOD/SCID/IL2rγ^{null} recipient. In the blood, Ter119$^+$ murine erythrocytes as well as hGPA$^+$ human erythrocytes were detected. mCD41a$^+$ murine platelets were also reconstituted. (C) Multilineage engraftment of human cells in the NOD/SCID/IL2rγ^{null} murine bone marrow. hCD33$^+$ myelomonocytic cells, hCD19$^+$ B cells, and hCD3$^+$ T cells were present. hGPA$^+$ erythroid cells and hCD41a$^+$ megakaryocytes were also seen in the nucleated cell gate of the bone marrow. (D, left) HLA-DR$^+$hCD11c$^+$ dendritic cells were detected in the spleen by a flow cytometric analysis. (Right) Immunohistochemical staining of CD11c in the spleen. CD11c$^+$ cells displayed dendritic cell morphology.

Thymocytes consisted of immature hCD4$^+$hCD8$^+$ double-positive (DP) T cells (Figure 3C) as well as small numbers of hCD4$^+$ or hCD8$^+$ single-positive (SP) mature T cells (Figure 4A, top panel), while hCD3$^+$ human T cells in spleen were mainly constituted of either hCD4$^+$ or hCD8$^+$ single positive T cells (Figure 4A, bottom panel). These data suggest that normal selection processes of T-cell development may occur in the recipients' thymi.

In the spleen, lymphoid follicle-like structures were seen (Figure 3D-E), where predominant hCD19$^+$ B cells were associated with surrounding scattered hCD3$^+$ T cells (Figure 3F). Development of mesenteric lymph nodes was also observed, where the similar follicle-like structures consisted of human B and T cells were present (not shown). In the bone marrow and the spleen, nucleated cells in each organ contained hCD34$^+$hCD19$^+$ pro-B cells, hCD10$^+$hCD19$^+$ immature B cells, and hCD19$^+$hCD20$^+$ mature B cells (Figure 4B). Figure 4C shows the expression of human immunoglobulins on hCD19$^+$ B cells. A significant fraction of hCD19$^+$ B cells expressed human IgM on their surface. A

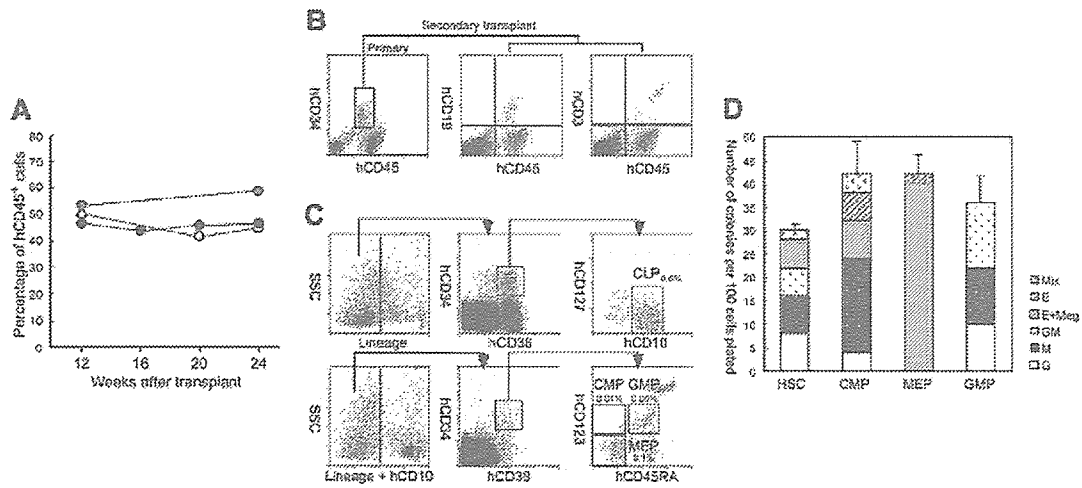

Figure 2. Purified Lin$^-$hCD34$^+$hCD38$^-$ CB cells reconstitute hematopoiesis via physiological intermediates, and display long-term reconstitution in the NOD/SCID/IL2rγ^{null} newborn system. (A) Serial evaluation of chimerism of human cells in peripheral blood of recipient mice injected with 2 × 10^4 Lin$^-$hCD34$^+$hCD38$^-$ CB cells. White, gray, and black dots represent 3 individual recipients. (B) hCD34$^+$ cells purified from a primary recipient marrow (left) were successfully engrafted into the secondary newborn recipients. hCD19$^+$ B cells (middle) and hCD3$^+$ T cells (right) in a representative secondary recipient is shown. (C) The Lin$^-$ bone marrow cells contained hCD34$^+$hCD38$^+$hCD10$^+$hCD127 (IL-7Rα)$^+$ CLPs (top row). In the Lin$^-$hCD10$^-$fraction, hCD34$^+$hCD38$^+$hCD45RA$^-$hCD123 (IL-3Rα)^{lo} CMPs, hCD34$^+$hCD38$^+$hCD45RA$^+$hCD123^{lo} GMPs, hCD34$^+$hCD38$^+$hCD45RA$^-$hCD123$^-$ MEPs were present. Each number for progenitors indicates percentages of hCD45$^+$ cells. SSC indicates side scatter. (D) Colony-forming activity of purified myeloid progenitor population in the methylcellulose assay. Representative data from 1 of 3 recipients are shown. Error bars represent standard deviation.

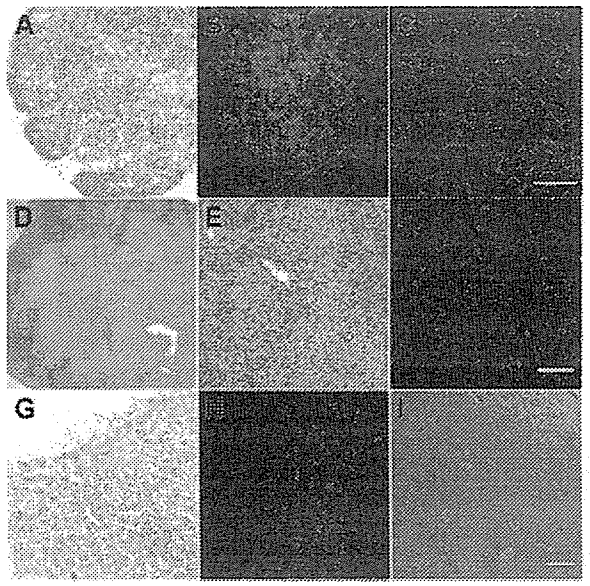

Figure 3. Histology of lymphoid organs in engrafted NOD/SCID/IL2rγ^{null} recipients. (A) The thymus showed an increased cellularity after reconstitution. (B) The thymus stained with anti-hCD3 (green) and anti-hCD19 (red) antibodies. (C) The thymus stained with anti-hCD4 (green) and anti-hCD8 (red) antibodies. The majority of thymocytes are doubly positive for hCD4 and hCD8. (D-E) Lymphoid follicle-like structures in the spleen of a recipient. (F) The lymphoid follicles mainly contained hCD19$^+$ B cells (red) that were surrounded by scattered hCD3$^+$ T cells (green). (G) Histology of the intestine in an engrafted NOD/SCID/IL2rγ^{null} recipient (left). (H) In the intestine, DAPI$^+$ (4′,6-diamidino-2-phenylindole)–nucleated cells (blue) contained both scattered hCD3$^+$ T cells (green) and human IgA$^+$ cells (red). (I) The DIC image of the same section shows that IgA$^+$ B cells were mainly found in the interstitial region of the intestinal mucosal layer. White bars inside panels represent 80 μm (C), 100 μm (F), and 20 μm (I).

fraction of cells expressing IgD were also observed in the blood and the spleen, suggesting that class switching occurred in these developing B cells. As reported in the Rag2$^{-/-}$ γc$^{-/-}$ mouse models,[10,12,14] hCD19$^+$IgA$^+$ B cells were detected in the bone marrow and the spleen in NOD/SCID/IL2rγ^{null} recipients. We then evaluated concentrations of human immunoglobulins in sera of mice given transplants of human Lin$^-$hCD34$^+$ CB cells by ELISA. In all sera from 3 NOD/SCID/IL2rγ^{null} recipients, a significant amount of IgG (257 ± 76 μg/mL) and IgM (600 ± 197 μg/mL) were detectable, whereas sera from the control NOD/SCID/β2m$^{-/-}$ mice contained lower levels of IgM (76 ± 41 μg/mL) and little or no IgG (Table S1, available on the *Blood* website; see the Supplemental Table link at the top of the online article). These data collectively suggest that class-switching can effectively occur in NOD/SCID/IL2rγ^{null} mice.

The intestinal tract is one of the major sites for supporting host defense against exogenous antigens. Since bone marrow and spleen hCD19$^+$ B cells contained a significant fraction of cells expressing IgA, we tested whether reconstitution of mucosal immunity could be achieved in the NOD/SCID/IL2rγ^{null} recipients. Immunohistologic analyses demonstrated that the intestinal tract of recipient mice contained significant numbers of cells expressing human IgA in addition to hCD3$^+$ T cells (Figure 3G-I). Thus, human CB cells could reconstitute cells responsible for both systemic and mucosal immunity in the NOD/SCID/IL2rγ^{null} newborn system.

Function of adaptive human immunity in engrafted NOD/SCID/IL2rγ^{null} mice

Five NOD/SCID/IL2rγ^{null} mice reconstituted with 3 independent human CB samples were immunized twice with ovalbumin (OVA) at 3 months after transplantation. Two weeks after immunization, sera were collected from these immunized mice, and were subjected to ELISA to quantify OVA-specific human IgG and IgM. As shown in Figure 5A, significant levels of OVA-specific human IgM and IgG were detected in all serum samples from immunized mice, but not in samples from nonimmunized engrafted mice. Thus, the adaptive human immune system properly functioned in the NOD/SCID/IL2rγ^{null} strain to produce antigen-specific human IgM and IgG antibodies.

We next tested the alloantigen-specific cytotoxic function of human T cells developed in NOD/SCID/IL2rγ^{null} recipients. hCD3$^+$ T cells isolated from the spleen of NOD/SCID/IL2rγ^{null} recipients were cultured with allogeneic B-LCL (TAK-LCL). We established 8 hCD4$^+$ and 10 hCD8$^+$ T-cell clones responding LCL-specific allogeneic antigens. We then estimated cytotoxic activity of these T-cell clones in the presence or absence of anti–HLA-DR and anti–HLA class I antibodies. We randomly chose 3 each of CD4 and CD8 clones for further analysis (Figure 5B). A ^{51}Cr release assay revealed that both hCD4$^+$ and hCD8$^+$ T cell clones exhibited cytotoxic activity against allogeneic TAK-LCL, whereas they showed no cytotoxicity against KIN-LCL, a cell line not sharing HLA classes I or II with TAK-LCL. Cytotoxic activity of hCD4$^+$

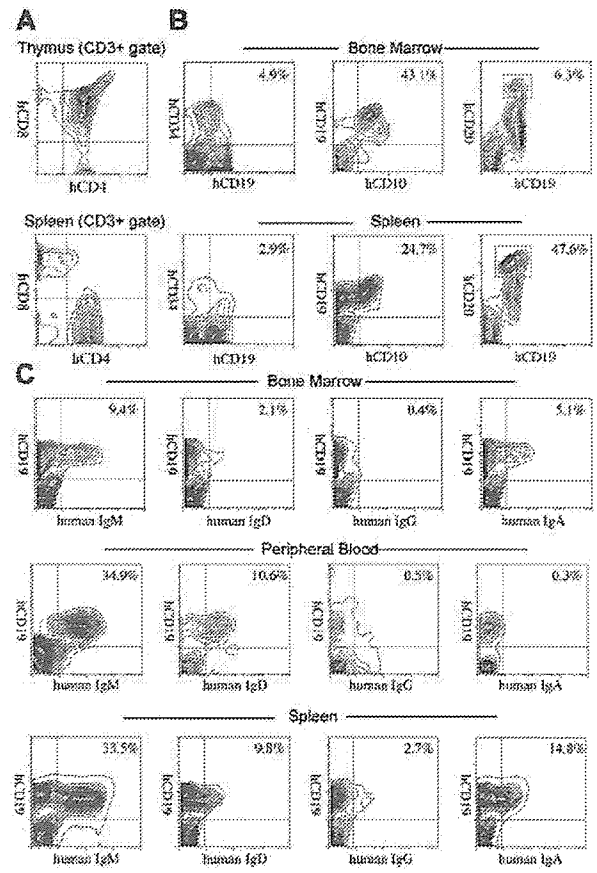

Figure 4. Development of lymphocytes in NOD/SCID/IL2rγ^{null} recipients. (A) The flow cytometric analysis of human T cells in recipients. The majority of cells in the thymus were hCD4$^+$hCD8$^+$ double-positive thymocytes (top). The CD3$^+$ spleen cells contained hCD4$^+$ or hCD8$^+$ single-positive mature T cells (bottom). (B) hCD34$^+$hCD19$^+$ pro-B, hCD10$^+$hCD19$^+$ pre-B, and hCD19$^+$hCD20^{hi} mature B cells were seen in different proportions in the bone marrow and the spleen of recipient mice. Numbers represent percentages within total nucleated cells. (C) B cells expressing each class of human immunoglobulin heavy chain were seen in the bone marrow, the peripheral blood (PB), or the spleen of engrafted NOD/SCID/IL2rγ^{null} mice. Numbers represent percentages out of nucleated cells.

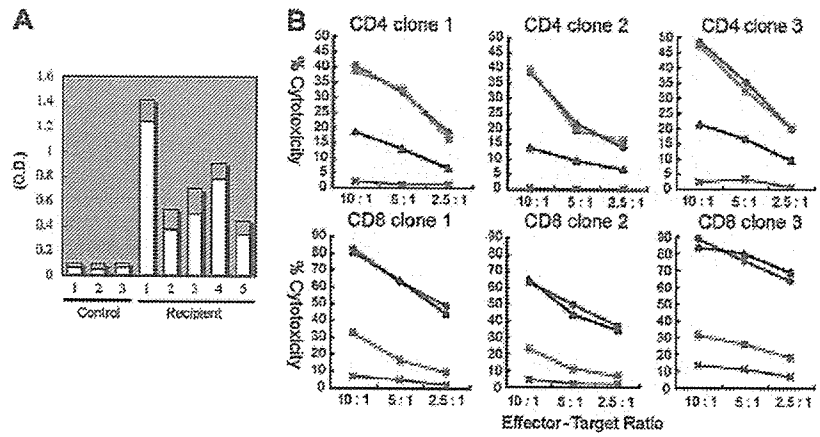

Figure 5. Functional analysis of human T and B cells developed in NOD/SCID/IL2rγ^{null} recipients. (A) Production of OVA-specific human immunoglobulins. Two weeks after immunization with OVA, sera of 5 independent recipients were sampled, and were evaluated for the concentration of OVA-specific human IgM (□) and IgG (▨) by ELISA. Sera of 3 nonimmunized NOD/SCID/IL2rγ^{null} recipients were used as controls. O.D. indicates optical density. (B) Cytotoxic activity of human T cells generated in NOD/SCID/IL2rg-null mice. hCD4+ and hCD8+ T-cell clones derived from the recipient spleen were cocultured with allogeneic target cells (TAK-LCLs). KIN-LCLs that do not share any HLA type with effector cells or TAK-LCLs (X) were used as negative controls. Both hCD4+ and hCD8+ T-cell lines displayed cytotoxic activity against TAK-LCL in a dose-dependent manner. In hCD4+ T-cell clones, this effect was blocked by anti–HLA-DR antibodies (▲), whereas in hCD8+ T-cell clones, the effect was blocked by anti–HLA class I antibodies (■). ◆ indicates cytotoxic response to TAK-LCLs without addition of antibodies.

and hCD8+ T cell clones was significantly inhibited by the addition of anti–HLA-DR and anti–HLA class I antibodies, respectively. These data clearly demonstrate that human CB-derived T cells can exhibit cytotoxic activity in an HLA-restricted manner.

Discussion

Xenogeneic transplantation models have been extensively used to study human hematopoiesis in vivo.[1,41,42] In the present study, we describe a new xenogeneic transplantation system that effectively supports human hemato-lymphoid development of all lineages for the long term.

NOD/SCID/IL2rγ^{null} newborns exhibited very efficient reconstitution of human hematopoietic and immune systems after intravenous injection of a relatively small number of CB cells. In our hands, NOD/SCID/IL2rγ^{null} newborns displayed a significantly higher chimerism of human blood cells compared with NOD/SCID/β2m$^{-/-}$ newborns under an identical transplantation setting (Table 1). This result directly shows that the IL2rγ^{null} mutation has a merit on human cell engraftment over the β2m$^{-/-}$ mutation.

One of the critical problems in the NOD/SCID strain for the use of recipients is that this mouse line possesses a predisposition to thymic lymphoma due to an endogenous ectropic provirus (Emv-30).[32] Because of this, NOD/SCID and NOD/SCID/β2m$^{-/-}$ mice have the short mean lifespan of 8.5 and 6 months, respectively, while NOD/SCID/IL2rγ^{null} mice did not develop thymic lymphoma surviving more than 15 months,[31] which allows a long-term experimentation.

In our study, NOD/SCID/IL2rγ^{null} newborns injected with 10^5 hCD34+ CB cells via a facial vein consistently displayed high levels of chimerism of human hematopoiesis (50%-80%; Table 1). This model is comparable to, or may be more efficient than the Rag2$^{-/-}$ γc$^{-/-}$ newborn model where intrahepatic injection of 0.4 to 1.2 × 10^5 hCD34+ CB cells generated variable levels of chimerism of human cells (5%-65%).[14] This slight difference of engraftment efficiency, however, could reflect the homing efficiency of HSCs by each injection route. The NOD/SCID/IL2rγ^{null} newborn model might be more efficient than the NOD/SCID/γ$_c^{-/-}$ adult model in which the majority of recipients showed approximately 30% chimerism of human cells after transplantation of 5 × 10^4 hCD34+ CB cells.[11] Although we did not test NOD/SCID/γ$_c^{-/-}$ newborns side by side in this study, we have found that the engraftment level of hCD34+ cells of human acute myelogenous leukemia is approximately 3-fold higher in newborns than adults in the NOD/SCID/IL2rγ^{null} strain (F.I., T.M., S.Y., M.Y., M.H., K.A., and L.D.S., manuscript in preparation). Therefore, it remains unclear whether the IL2rγ^{null} mutation has a significant advantage over the truncated γc mutation[11] for human cell engraftment. It is still possible that the improved engraftment efficiencies in the NOD/SCID/IL2rγ^{null} newborn system as compared to those in the NOD/SCID/γ$_c^{-/-}$ adult system reflect the age-dependent maturation of the xenogeneic barrier.

The Rag2$^{-/-}$ γc$^{-/-}$ newborn and NOD/SCID/γ$_c^{-/-}$ adult models have provided definitive evidences that functional T cells, B cells, and dendritic cells can develop from hematopoietic progenitor cells in immunodeficient mice. Class-switching of immunoglobulin in CB-derived B cells properly occurred in the NOD/SCID/IL2rγ^{null} but not in the NOD/SCID/β2m$^{-/-}$ newborns (Table S1), further confirming the advantage of the NOD/SCID/IL2rγ^{null} model. We also showed that, consistent with a previous report using the Rag2$^{-/-}$ γc$^{-/-}$ model,[14] human T and B cells developed in NOD/SCID/IL2rγ^{null} mice are capable of mounting antigen-specific immune responses. Interestingly, human T and B cells migrated into murine lymphoid organs and into the intestinal tissues to collaborate in forming lymphoid organ structures. Furthermore, we found that IgA-secreting human B cells can develop in the murine intestine, suggesting that human mucosal immunity could be generated. Thus, the cellular interaction and the lymphocyte homing could occur at least to some extent across the xenogenic barrier in this model. It is also of interest that developing human cells in the thymus displayed normal distribution of SP and DP cells (Figure 4A), and that mature human T cells displayed cytotoxic functions in an HLA-dependent manner (Figure 5B). This suggests that positive and/or negative selection of human T cells could occur in NOD/SCID/IL2rγ^{null} recipients. Thymic epithelial cells in recipients reacted with anti-murine but not anti-human centromere probes in a FISH assay (F.I. and M.H., unpublished data, September 2004), confirming their recipient's origin. Thus, it remains unclear how these human T cells effectively educated and developed in murine thymus. It is also possible that human mature T cells developed by extrathymic education and selection.

Our data directly show that the most primitive hCD34+hCD38− CB cells are capable of generating the human myeloerythroid system in addition to the immune system in the NOD/SCID/IL2rγ^{null} recipients. The emergence of circulating hCD33+ myelomonocytic cells after transplantation of human CB cells has been reported in the NOD/SCID/β2m$^{-/-}$ newborn[33] and the NOD/SCID/γ$_c^{-/-}$ adult[11] systems. Development of human erythropoiesis, however, has not been obtained in previous models,

although it has been reported that NOD/SCID mice can support terminal maturation of hCD71$^+$ erythroblasts that were induced ex vivo from human HSCs by culturing with human cytokines.[43] We showed for the first time that human erythropoiesis and thrombopoiesis can develop in mice from primitive hCD34$^+$hCD38$^-$ cells, as evidenced by the presence of erythroblasts and megakaryocytes in the bone marrow and of circulating erythrocytes and platelets in NOD/SCID/IL2rγ^{null} recipients. It is important to note that the hCD34$^+$hCD38$^-$ CB HSC population generated myeloid- and lymphoid-restricted progenitor populations such as CMPs, GMPs, MEPs, and CLPs in the bone marrow (Figure 2E-F). Thus, the NOD/SCID/IL2rγ^{null} microenvironment might be able to support physiological steps of myelopoiesis and lymphopoiesis initiating from the primitive HSC stage.

In summary, we show that the NOD/SCID/IL2rγ^{null} newborn system efficiently supports hemato-lymphoid development from primitive human HSCs, passing through physiological developmental intermediates. It also can support development of human systemic and mucosal immunity, and therefore may be useful to use human immunity to produce immunoglobulins or experimental vaccines. The NOD/SCID/IL2rγ^{null} newborn system might also serve as an efficient tool for understanding malignant hematopoiesis in humans, since the analysis of human leukemogenesis has mainly been dependent upon the NOD/SCID adult mouse system.[44-46] Our model might also be useful to reproduce the transforming process of human hematopoietic cells, as transplanted murine hematopoietic progenitor and stem cells can develop leukemia by transducing oncogenic fusion genes in syngeneic mouse models.[47,48] Thus, the use of this system should open a more efficient way to analyze normal and malignant human hematopoiesis.

Acknowledgments

We thank Bruce Gott and Lisa Burzenski for excellent technical assistance, and Dr Sato and other staff at Fukuoka Cord Blood Bank for preparation of CB.

References

1. Greiner DL, Hesselton RA, Shultz LD. SCID mouse models of human stem cell engraftment. Stem Cells. 1998;16:166-177.
2. McCune JM, Namikawa R, Kaneshima H, Shultz LD, Lieberman M, Weissman IL. The SCID-hu mouse: murine model for the analysis of human hematolymphoid differentiation and function. Science. 1988;241:1632-1639.
3. Mosier DE, Gulizia RJ, Baird SM, Wilson DB. Transfer of a functional human immune system to mice with severe combined immunodeficiency. Nature. 1988;335:256-259.
4. Kaneshima H, Namikawa R, McCune JM. Human hematolymphoid cells in SCID mice. Curr Opin Immunol. 1994;6:327-333.
5. Pflumio F, Izac B, Katz A, Shultz LD, Vainchenker W, Coulombel L. Phenotype and function of human hematopoietic cells engrafting immune-deficient CB17-severe combined immunodeficiency mice and nonobese diabetic-severe combined immunodeficiency mice after transplantation of human cord blood mononuclear cells. Blood. 1996;88:3731-3740.
6. Shultz LD, Lang PA, Christianson SW, et al. NOD/LtSz-Rag1null mice: an immunodeficient and radioresistant model for engraftment of human hematolymphoid cells, HIV infection, and adoptive transfer of NOD mouse diabetogenic T cells. J Immunol. 2000;164:2496-2507.
7. Goldman JP, Blundell MP, Lopes L, Kinnon C, Di Santo JP, Thrasher AJ. Enhanced human cell engraftment in mice deficient in RAG2 and the common cytokine receptor gamma chain. Br J Haematol. 1998;103:335-342.
8. Greiner DL, Shultz LD, Yates J, et al. Improved engraftment of human spleen cells in NOD/LtSz-scid/scid mice as compared with C.B-17-scid/scid mice. Am J Pathol. 1995;146:888-902.
9. Yoshino H, Ueda T, Kawahata M, et al. Natural killer cell depletion by anti-asialo GM1 antiserum treatment enhances human hematopoietic stem cell engraftment in NOD/Shi-scid mice. Bone Marrow Transplant. 2000;26:1211-1216.
10. Kollet O, Peled A, Byk T, et al. beta2 microglobulin-deficient (B2m(null)) NOD/SCID mice are excellent recipients for studying human stem cell function. Blood. 2000;95:3102-3105.
11. Ito M, Hiramatsu H, Kobayashi K, et al. NOD/SCID/gamma(c)(null) mouse: an excellent recipient mouse model for engraftment of human cells. Blood. 2002;100:3175-3182.
12. Hiramatsu H, Nishikomori R, Heike T, et al. Complete reconstitution of human lymphocytes from cord blood CD34+ cells using the NOD/SCID/gammacnull mice model. Blood. 2003;102:873-880.
13. Leonard WJ. Cytokines and immunodeficiency diseases. Nat Rev Immunol. 2001;1:200-208.
14. Traggiai E, Chicha L, Mazzucchelli L, et al. Development of a human adaptive immune system in cord blood cell-transplanted mice. Science. 2004; 304:104-107.
15. Ohbo K, Suda T, Hashiyama M, et al. Modulation of hematopoiesis in mice with a truncated mutant of the interleukin-2 receptor gamma chain. Blood. 1996;87:956-967.
16. Cao X, Shores EW, Hu-Li J, et al. Defective lymphoid development in mice lacking expression of the common cytokine receptor gamma chain. Immunity. 1995;2:223-238.
17. DiSanto JP, Muller W, Guy-Grand D, Fischer A, Rajewsky K. Lymphoid development in mice with a targeted deletion of the interleukin 2 receptor gamma chain. Proc Natl Acad Sci U S A. 1995; 92:377-381.
18. Asao H, Takeshita T, Ishii N, Kumaki S, Nakamura M, Sugamura K. Reconstitution of functional interleukin 2 receptor complexes on fibroblastoid cells: involvement of the cytoplasmic domain of the gamma chain in two distinct signaling pathways. Proc Natl Acad Sci U S A. 1993;90: 4127-4131.
19. Takeshita T, Asao H, Ohtani K, et al. Cloning of the gamma chain of the human IL-2 receptor. Science. 1992;257:379-382.
20. Russell SM, Keegan AD, Harada N, et al. Interleukin-2 receptor gamma chain: a functional component of the interleukin-4 receptor. Science. 1993;262:1880-1883.
21. Noguchi M, Nakamura Y, Russell SM, et al. Interleukin-2 receptor gamma chain: a functional component of the interleukin-7 receptor. Science. 1993;262:1877-1880.
22. Kondo M, Takeshita T, Higuchi M, et al. Functional participation of the IL-2 receptor gamma chain in IL-7 receptor complexes. Science. 1994; 263:1453-1454.
23. Kondo M, Takeshita T, Ishii N, et al. Sharing of the interleukin-2 (IL-2) receptor gamma chain between receptors for IL-2 and IL-4. Science. 1993; 262:1874-1877.
24. Ferrag F, Pezet A, Chiarenza A, et al. Homodimerization of IL-2 receptor beta chain is necessary and sufficient to activate Jak2 and downstream signaling pathways. FEBS Lett. 1998;421: 32-36.
25. Reichel M, Nelson BH, Greenberg PD, Rothman PB. The IL-4 receptor alpha-chain cytoplasmic domain is sufficient for activation of JAK-1 and STAT6 and the induction of IL-4-specific gene expression. J Immunol. 1997;158:5860-5867.
26. Shultz LD, Lyons BL, Burzenski LM, et al. Human lymphoid and myeloid cell development in NOD/LtSz-scid IL2rgnull mice engrafted with mobilized human hematopoietic stem cells. J Immunol. 2005;174:6477-6489.
27. Sands MS, Barker JE, Vogler C, et al. Treatment of murine mucopolysaccharidosis type VII by syngeneic bone marrow transplantation in neonates. Lab Invest. 1993;68:676-686.
28. Manz MG, Miyamoto T, Akashi K, Weissman IL. Prospective isolation of human clonogenic common myeloid progenitors. Proc Natl Acad Sci U S A. 2002;99:11872-11877.
29. Galy A, Travis M, Cen D, Chen B. Human T, B, natural killer, and dendritic cells arise from a common bone marrow progenitor cell subset. Immunity. 1995;3:459-473.
30. LeBien TW. Fates of human B-cell precursors. Blood. 2000;96:9-23.
31. Yanai F, Ishii E, Kojima K, et al. Essential roles of perforin in antigen-specific cytotoxicity mediated by human CD4+ T lymphocytes: analysis using the combination of hereditary perforin-deficient effector cells and Fas-deficient target cells. J Immunol. 2003;170:2205-2213.
32. Prochazka M, Gaskins HR, Shultz LD, Leiter EH. The nonobese diabetic scid mouse: model for spontaneous thymomagenesis associated with immunodeficiency. Proc Natl Acad Sci U S A. 1992;89:3290-3294.
33. Ishikawa F, Livingston AG, Wingard JR, Nishikawa S, Ogawa M. An assay for long-term engrafting human hematopoietic cells based on newborn NOD/SCID/beta2-microglobulin(null) mice. Exp Hematol. 2002;30:488-494.
34. Kina T, Ikuta K, Takayama E, et al. The monoclonal antibody TER-119 recognizes a molecule associated with glycophorin A and specifically marks the late stages of murine erythroid lineage. Br J Haematol. 2000;109:280-287.
35. Okuno Y, Iwasaki H, Huettner CS, et al. Differential regulation of the human and murine CD34 genes in hematopoietic stem cells. Proc Natl Acad Sci U S A. 2002;99:6246-6251.
36. Craig W, Kay R, Cutler RL, Lansdorp PM. Expression of Thy-1 on human hematopoietic progenitor cells. J Exp Med. Vol. 177; 1993:1331-1342.
37. Terstappen LW, Huang S, Safford M, Lansdorp

PM, Loken MR. Sequential generations of hematopoietic colonies derived from single nonlineage-committed CD34+CD38- progenitor cells. Blood. 1991;77:1218-1227.

38. Akashi K, Traver D, Miyamoto T, Weissman IL. A clonogenic common myeloid progenitor that gives rise to all myeloid lineages. Nature. 2000;404:193-197.
39. Kondo M, Weissman IL, Akashi K. Identification of clonogenic common lymphoid progenitors in mouse bone marrow. Cell. 1997;91:661-672.
40. Akashi K, Richie LI, Miyamoto T, Carr WH, Weissman IL. B lymphopoiesis in the thymus. J Immunol. 2000;164:5221-5226.
41. Zanjani ED. The human sheep xenograft model for the study of the in vivo potential of human HSC and in utero gene transfer. Stem Cells. 2000;18:151.
42. Stier S, Cheng T, Forkert R, et al. Ex vivo targeting of p21Cip1/Waf1 permits relative expansion of human hematopoietic stem cells. Blood. 2003;102:1260-1266.
43. Neildez-Nguyen TM, Wajcman H, Marden MC, et al. Human erythroid cells produced ex vivo at large scale differentiate into red blood cells in vivo. Nat Biotechnol. 2002;20:467-472.
44. Lumkul R, Gorin NC, Malehorn MT, et al. Human AML cells in NOD/SCID mice: engraftment potential and gene expression. Leukemia. 2002;16:1818-1826.
45. Hope KJ, Jin L, Dick JE. Acute myeloid leukemia originates from a hierarchy of leukemic stem cell classes that differ in self-renewal capacity. Nat Immunol. 2004;5:738-743.
46. Bonnet D, Dick JE. Human acute myeloid leukemia is organized as a hierarchy that originates from a primitive hematopoietic cell. Nat Med. 1997;3:730-737.
47. Cozzio A, Passegue E, Ayton PM, Karsunky H, Cleary ML, Weissman IL. Similar MLL-associated leukemias arising from self-renewing stem cells and short-lived myeloid progenitors. Genes Dev. 2003;17:3029-3035.
48. Huntly BJ, Shigematsu H, Deguchi K, et al. MOZ-TIF2, but not BCR-ABL, confers properties of leukemic stem cells to committed murine hematopoietic progenitors. Cancer Cell. 2004;6:587-596.

Mobilization of Human Lymphoid Progenitors after Treatment with Granulocyte Colony-Stimulating Factor[1]

Rie Imamura,[3]*†‡ Toshihiro Miyamoto,[2,3]† Goichi Yoshimoto,† Kenjiro Kamezaki,*† Fumihiko Ishikawa,† Hideho Henzan,*† Koji Kato,† Ken Takase,*† Akihiko Numata,*† Koji Nagafuji,† Takashi Okamura,‡ Michio Sata,‡ Mine Harada,† and Shoichi Inaba[4]*

Hemopoietic stem and progenitor cells ordinarily residing within bone marrow are released into the circulation following G-CSF administration. Such mobilization has a great clinical impact on hemopoietic stem cell transplantation. Underlying mechanisms are incompletely understood, but may involve G-CSF-induced modulation of chemokines, adhesion molecules, and proteolytic enzymes. We studied G-CSF-induced mobilization of $CD34^+CD10^+CD19^-Lin^-$ and $CD34^+CD10^+CD19^+Lin^-$ cells (early B and pro-B cells, respectively). These mobilized lymphoid populations could differentiate only into B/NK cells or B cells equivalent to their marrow counterparts. Mobilized lymphoid progenitors expressed lymphoid- but not myeloid-related genes including the G-CSF receptor gene, and displayed the same pattern of Ig rearrangement status as their bone marrow counterparts. Decreased expression of VLA-4 and CXCR-4 on mobilized lymphoid progenitors as well as multipotent and myeloid progenitors indicated lineage-independent involvement of these molecules in G-CSF-induced mobilization. The results suggest that by acting through multiple *trans*-acting signals, G-CSF can mobilize not only myeloid-committed populations but a variety of resident marrow cell populations including lymphoid progenitors. *The Journal of Immunology,* **2005, 175: 2647–2654.**

Hemopoietic stem and progenitor cells (HPC),[5] which usually reside within bone marrow (BM), can be released into circulation after treatment with cytokines, cytotoxic agents, or both (1). Among a number of agents, G-CSF is the cytokine most commonly used clinically to mobilize HPC in a variety of transplantation settings because of its potency and lack of serious toxicity. Especially in allogeneic stem cell transplantation, G-CSF-mobilized peripheral blood stem and progenitor cells (PBPC) now are replacing marrow-derived HPC as a stem cell source.

G-CSF acts by binding to its receptor (G-CSFR), a member of the class I cytokine receptor family expressed on various hemopoietic cells such as stem cells, multipotent progenitors, myeloid-committed progenitors, neutrophils, and monocytes (2–4). Liu et al. (5) showed a significant effect of G-CSF signals on HPC mobilization by demonstrating that mice deficient in G-CSFR failed to mobilize HPC in response to G-CSF. Conversely, they also reported that chimeric mice with both wild-type and deleted G-CSFR can mobilize equal numbers of HPC with or without the receptor in response to G-CSF (6). Thus, G-CSFR expression on HPC may not be crucial for their mobilization by G-CSF. These data indicate that G-CSF can induce HPC mobilization by pathways not limited to transmittal of G-CSF signals directly onto the target cells. Recent insights using experimental animal models are provided suggesting that HPC mobilization by G-CSF could be mediated by indirect effects involving generation of multiple *trans*-acting signals in the marrow microenvironment (7–11). Proteolytic enzymes such as neutrophil elastase, cathepsin G, and matrix metalloproteinase (MMP)-9 released from the activated neutrophils and monocytes can degrade and/or inactivate the adhesion molecules such as VCAM-1/VLA-4, chemokines such as stromal-derived factor (SDF)-1/CXCR-4, and soluble Kit ligand, resulting in the disruption of contact between HPC and the BM microenvironment. HPC then would be released to migrate into peripheral blood (PB). However, details of the mechanisms of HPC mobilization by G-CSF are not yet fully understood, especially in humans.

Marrow is the primary lymphohematopoietic organ where B lymphoid lineage development occurs. Under ordinary steady-state conditions, immature lymphoid progenitors in various stages of differentiation as well as multipotent and myeloid progenitors are confined to BM microenvironments in which they undergo further differentiation; then the mature cells leave the BM and circulate in the blood. In this context, considering the broad spectrum of target cells affected by G-CSF and involvement of changes affecting adhesion molecules in HPC mobilization, G-CSF might be expected to mobilize not only G-CSFR-possessing cells but a variety of cell populations including lymphoid cells and nonhematopoietic cells residing within the BM. Accordingly, we evaluated populations of G-CSF-mobilized blood cells in detail using multicolor flow cytometry to better understand the mechanism of G-CSF-induced mobilization in humans. We identified small but significant populations possessing immature lymphoid phenotypes such as

*Blood Transfusion Service, Kyushu University Hospital, †Medicine and Biosystemic Science, Kyushu University Graduate School of Medical Sciences, and ‡Second Department of Internal Medicine, Kurume University School of Medicine, Fukuoka, Japan

Received for publication August 2, 2004. Accepted for publication May 27, 2005.

The costs of publication of this article were defrayed in part by the payment of page charges. This article must therefore be hereby marked *advertisement* in accordance with 18 U.S.C. Section 1734 solely to indicate this fact.

[1] This work was supported in part by a Grant-in-Aid from the Ministry and Education, Science, Sports, and Culture in Japan (14704034) (to T.M.).

[2] Address correspondence and reprint request to Dr. Toshihiro Miyamoto at the current address: Center for Cellular and Molecular Medicine, Kyushu University Hospital, 3-1-1 Maidashi, Higashi-ku, Fukuoka 812-8582, Japan. E-mail address: toshmiya@inmed1.med.kyushu-u.ac.jp

[3] R.I. and T.M. contributed equally to the research described in this paper.

[4] Current address: Kanagawa Red Cross Hospital Center, 219-3 Gumisawa-cho, Totsuka-ku, Yokohama 245-8585, Japan.

[5] Abbreviations used in this paper: HPC, hematopoietic stem and progenitor cells; BM, bone marrow; PBPC, peripheral blood stem and progenitor cells; G-CSFR, G-CSF receptor; MMP, matrix metalloproteinase; SDF, stromal-derived factor; PB, peripheral blood; MNC, mononuclear cells; MPP, multipotent progenitor cells; SCF, stem cell factor; FL, flt3/flk2-ligand; LTC-IC, long-term culture initiating-cell; CLP, common lymphoid progenitors; MFI, mean fluorescence intensity.

0022-1767/05/$02.00

$CD34^+CD10^+CD19^-$ and $CD34^+CD10^+CD19^+$ cells among G-CSF-mobilized cells in blood; these have been defined as early B and pro-B cells in the BM, respectively. The mobilized $CD34^+CD10^+CD19^-$ and $CD34^+CD10^+CD19^+$ cells are capable of differentiation into B/NK cells or B cells that are equivalent to their BM counterparts. Furthermore, these mobilized lymphoid progenitors express lymphoid-related genes but not myeloid-affiliated genes including G-CSFR. In addition, Ig gene rearrangements were detected in these mobilized progenitors. Expression of adhesion molecules such as VLA-4 and CXCR-4 on the mobilized lymphoid progenitors as well as multipotent and myeloid progenitors was down-regulated compared with their steady-state BM and even G-CSF-treated BM counterparts. Thus, G-CSF can mobilize not only myeloid progenitors but also early B and pro-B progenitor cells by modulation of adhesion molecules in a lineage-independent manner. These findings also support the hypothesis that G-CSF can mediate HPC mobilization indirectly in humans as well as mice.

Materials and Methods

Patients

G-CSF-mobilized PB samples were collected from 82 healthy allogeneic PBPC donors who received G-CSF (Filgrastim; Kirin) s.c. at 400 $\mu g/m^2$ per day for 5 days. G-CSF-treated BM samples also were collected from three of these volunteer donors on day 5 of G-CSF administration. Steady-state BM and PB samples were collected from 14 and 34 healthy adults, respectively. Informed consent was obtained from all subjects.

Cell preparation and staining

PB and BM mononuclear cells (MNC) were prepared by gradient centrifugation. For analysis of myeloid progenitor cells, cell samples were stained with a Cy5-PE-conjugated lineage (Lin) mixture (anti-CD3, -CD4, -CD8, -CD11b, -CD16, -CD20, -CD56, and glycophorin A; Caltag Laboratories), FITC-conjugated anti-CD13 (BD Pharmingen), PE-conjugated anti-CD33 (BD Pharmingen), allophycocyanin-conjugated anti-CD34 (BD Pharmingen), and biotin-conjugated anti-CD38 (Caltag Laboratories) Abs. B lymphoid progenitors were stained with the same Cy5-PE-conjugated lineage mixture followed by FITC-conjugated anti-CD10 (Ancell), PE-conjugated anti-CD19 (BD Pharmingen), and anti-CD38 and -CD34 as described above. For analysis of T-lymphoid progenitors, Lin^- cells were stained with FITC-conjugated anti-CD7 (BD Pharmingen), PE-conjugated anti-CD2 (BD Pharmingen), and anti-CD38 and -CD34 as described above. Streptavidin-conjugated Cy7-allophycocyanin (Caltag Laboratories) were used for visualization of biotinylated Abs. Nonviable cells were excluded by propidium iodide staining. Expression of adhesion molecules was detected on progenitors staining by PE-conjugated anti-CXCR-4, VLA-4, and c-Kit (BD Pharmingen), together with anti-CD10 or -CD13 and anti-CD38 and -CD34 as described above.

For sorting cells, $CD34^+$ cells were enriched from MNC using immunomagnetic beads according to the manufacturer's instructions ($CD34^+$ selection kit; Miltenyi Biotec) followed by staining specific for progenitors of each lineage as described above. $CD34^+CD38^{-/low}CD13^-CD10^-CD19^-Lin^-$ multipotent progenitor cells (MPP), $CD34^+CD38^+CD13^+CD10^-CD19^-Lin^-$ myeloid progenitor cells, $CD34^+CD38^+CD10^+CD19^-CD13^-Lin^-$ early B cells, and $CD34^+CD38^+CD10^+CD19^+CD13^-Lin^-$ pro-B cells were sorted by a highly modified triple laser (488-nm argon laser, 633-nm helium-neon laser, and UV laser) FACS (FACSVantage SE; BD Pharmingen). Five-color sorting using both positive and negative gates in multiple channels usually gives rise to cells with >98% purity, avoiding cosorted cells stained in a nonspecific manner. The sorted cells were subjected to an additional round of sorting using the same gate to eliminate contaminating cells and doublets (12).

In vivo and in vitro assays to determine differentiation potential

Clonogenic progenitor assay was performed using a methylcellulose culture system as reported previously (12, 13). Cells also were cultured on the irradiated Sys-1 or MS-5 stromal cell layers (14, 15). Human cytokines such as stem cell factor (SCF) (20 ng/ml), IL-3 (30 ng/ml), IL-2 (50 ng/ml), GM-CSF (20 ng/ml), erythropoietin (2 U/ml), thrombopoietin (20 ng/ml; Kirin), IL-7 (20 ng/ml), flt3/flk2-ligand (FL; 10 ng/ml), and IL-11 (10 ng/ml; R&D Systems) were added at the start of the culture.

Long-term culture initiating-cell (LTC-IC) assays were performed in human long-term culture medium (Myelocult H5100; StemCell Technologies) supplemented with hydrocortisone on irradiated M2-10B4 stromal layers as described previously (13). At 6 wk of culture on the stromal layers, cells were transferred to the methylcellulose medium, and colonies were counted 14 days later.

For limiting dilution analysis, variable numbers of double-sorted early B cells were deposited on the MS-5 stromal cell layers in the presence of IL-7, IL-11, SCF, FL, and IL-2, using an automatic cell deposition unit system (BD Pharmingen). All cultures were incubated at 37°C in a humidified atmosphere including 7% CO_2.

For reconstitution assays, FACS-sorted cells were injected into irradiated (350 rad) NOD/SCID/β_2-microglobulin knockout (NOD/SCID/$\beta 2^{-/-}$) mice as described previously (16). At 6–8 wk after transplantation, BM and spleen were collected for analysis by flow cytometery. Cells were stained with mAbs to human leukocyte differentiation Ags, including CD45, CD19, CD10, CD15, CD56, and CD3.

Gene expression profile by RT-PCR

To examine gene expression profile of each population, total RNA was purified from 1000 double-sorted cells and was amplified by RT-PCR (12). The primer sequences were reported previously (13). PCR products were electrophoresed on an ethidium bromide-stained 2.0% agarose gel. PCR amplification was repeated at least twice for at least two separately prepared samples.

PCR analysis of IgH gene rearrangement

To analyze IgH gene rearrangements status of each population, DNA was extracted from double-sorted 5000 cells, and PCR amplification of VDJ_H and DJ_H rearrangement was performed as described previously (17, 18). This PCR analysis can detect incomplete DJ_H rearrangements of IgH gene with a mixtures of upstream D_H primers and a consensus J_H primer, resulting in a ladder of different sized products ranging from 70 to 100 bp depending on the length of the DJ_H rearrangements. The GAPDH gene primers were used as control for DNA integrity.

Statistical analyses

Levels of significance were measured using paired t test. $p < 0.05$ was considered significant.

Results

Phenotypic analysis

Using a five-color cell sorter, we analyzed the distribution of each cell population including multipotent, myeloid, and lymphoid progenitors. Under unstimulated conditions, few $CD34^+Lin^-$ cells circulated in the periphery (0.023 ± 0.014% of MNC; $n = 34$), whereas the number of circulating $CD34^+Lin^-$ cells increased up to 0.59 ± 0.35% of MNC after G-CSF administration (Table I). $CD34^+Lin^-$ fractions are subdivided into two fractions according to expression of CD38: $CD34^+CD38^{-/low}Lin^-$ fractions contain hemopoietic stem cells with multipotent, self-renewing capacity, whereas $CD34^+CD38^+Lin^-$ cells include lineage-committed progenitors that have lost self-renewing capacity (Fig. 1*A*) (13).

In BM, G-CSF administration increased the number of MNC up to ~2.4-fold, with dominant expansion of myeloid-committed progenitors and mature granulocytes/macrophages; this reflected a relatively reduced percentage of the primitive $CD34^+CD38^{-/low}Lin^-$ population (Table I). Although $CD34^+CD38^{-/low}Lin^-$ cells were mobilized into the periphery by G-CSF, their percentage was significantly lower than in steady-state BM (Table I). Following G-CSF, most $CD34^+$ cells were $CD13^+CD38^+$ myeloid-committed progenitors; myeloid progenitors constituted 92.30 ± 3.76% and 96.70 ± 6.62% of $CD34^+CD38^+Lin^-$ cells in BM and PB, respectively (Table I and Fig. 1*B*). These data showed that myeloid-committed progenitors expanded within BM and were the main population mobilized by G-CSF administration.

Lymphoid progenitors mobilized by G-CSF

Under ordinary conditions, after commitment to the B lymphoid differentiation pathway, $CD34^+CD38^{-/low}Lin^-$ MPP cells become $CD34^+CD38^+CD10^+CD19^-CD20^-$ early B cells or common lymphoid progenitors (CLP) (14, 19) and differentiate within

Table I. *Subsets of $CD34^+CD38^+Lin^-$ fraction among cells from steady-state BM, G-CSF-treated marrow, and G-CSF-mobilized PB*[a]

	Steady-State PB (n = 34)	Steady-State BM (n = 14)	G-CSF-Treated BM (n = 3)	G-CSF-Mobilized PB (n = 82)
% $CD34^+Lin^-$ cells/MNC	0.023 ± 0.014	1.49 ± 0.62	1.03 ± 0.12	0.59 ± 0.35[b]
% $CD34^+CD38^-Lin^-$/MNC	ND	0.15 ± 0.072	0.078 ± 0.015	0.060 ± 0.036[b]
% $CD13^+/CD34^+CD38^+Lin^-$	80.51 ± 7.59	89.21 ± 6.91	92.3 ± 3.76	96.70 ± 6.62[b]
% $CD10^+CD19^+/CD34^+CD38^+Lin^-$	ND	8.93 ± 5.37	5.52 ± 3.04	1.49 ± 1.30[b]
% $CD10^+CD19^-/CD34^+CD38^+Lin^-$	ND	0.82 ± 0.56	0.44 ± 0.11	0.14 ± 0.09[b]

[a] Data are expressed as mean ± SD. ND, not detected.
[b] Significantly different from steady-state BM ($p < 0.05$).

the BM through a $CD34^+CD38^+CD10^+CD19^+CD20^-$ pro-B phenotype into a $CD34^{-/low}CD38^+CD10^-CD19^+CD20^+$ pre-B phenotype (Fig. 1*A*) (20). Then mature B cells are released from the BM into the circulation. In our analysis, early B and pro-B cells were undetectable in the PB of 34 healthy volunteers (data not shown). In the steady-state BM, early B cells and pro-B cells comprised 0.82 ± 0.56% and 8.93 ± 5.37% of $CD34^+CD38^+Lin^-$ cells, respectively (n = 14; Table I). Following G-CSF administration, despite the relatively reduced percentage of lymphoid progenitors reflecting expansion of myeloid lineage cells, absolute numbers of early B and pro-B cells in BM were not significantly different from those in steady-state BM (Table I).

Surprisingly, the G-CSF-mobilized PB contained small but significant populations possessing the same lymphoid phenotypes as BM early B and pro-B cells in the $CD34^+CD38^+Lin^-$ fractions: $CD10^+CD19^-$ and $CD10^+CD19^+$ cells were detectable in 60 and 80 of 82 cases, respectively. A representative FACS analysis is shown in Fig. 1*B*. These $CD10^+CD19^-$ and $CD10^+CD19^+$ cells constituted 0.14 ± 0.09% (0–0.68%) and 1.49 ± 1.30% (0–8.58%) of $CD34^+CD38^+Lin^-$ cells, and ~0.001% and 0.01% of G-CSF-mobilized PB MNC, respectively (Table I). The percentage of circulating lymphoid progenitors was 10 and 6 times less than that in steady-state BM and in G-CSF-treated BM, respectively. T-lineage progenitor coexpressing CD34 and CD7 or CD2 was undetectable in the G-CSF-mobilized PB (data not shown). These lymphoid progenitors were doubly sorted and subjected to analyses of differentiation capacity and gene expression profiles as follows.

Change in expression of adhesion molecules during G-CSF mobilization

We next evaluated expression of c-Kit and adhesion molecules such as VLA-4 and CXCR-4 on different progenitors during G-CSF administration. Fig. 2 shows the mean fluorescence intensity (MFI) for these molecules among MPP, myeloid progenitors, and lymphoid progenitors.

Under physiological conditions, c-Kit was expressed at a low level on the BM $CD34^+CD38^{-/low}Lin^-$ primitive MPP. Its expression was up-regulated in myeloid progenitors but shut down in $CD10^+$ lymphoid progenitors (Fig. 2*A*); these results are consistent with those reported previously (14, 21). CXCR-4, a receptor for SDF-1 that is critical for homing of HPC as well as B lymphopoiesis (22), was highly expressed on lymphoid progenitors, whereas MPP and myeloid progenitors showed low CXCR-4 expression (Fig. 2*B*). VLA-4 was expressed on all three types of progenitors; frequency of expression did not differ significantly among them (Fig. 2*C*).

Following G-CSF administration, MFI for c-Kit expression on MPP and myeloid progenitors was decreased in PB compared with that in steady-state BM (Fig. 2*A*). In contrast, lymphoid progenitors showed low to absent c-Kit expression, and MFI between the tissues was not different. As shown in Fig. 2, *B* and *C*, MFI for

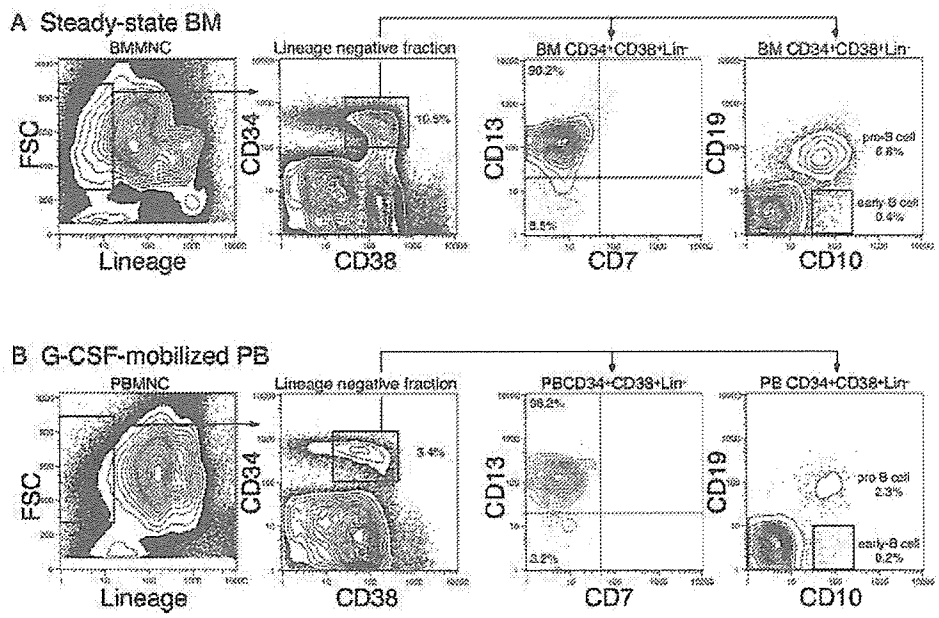

FIGURE 1. Five-color flow cytometric analyses of BM (*A*) and G-CSF-mobilized PB cells (*B*). Cells first were gated by lack of expression of lineage-related Ags. Most $CD34^+CD38^+$ BM cells are $CD13^+$ myeloid-committed cells. Small lymphoid-committed populations such as $CD10^+CD19^-$ early B and $CD10^+CD19^+$ pro-B cells exist in the $CD34^+CD38^+$ fraction but are absent from the peripheral circulation under steady-state condition (*A*). Following G-CSF administration, minor populations possessing the same phenotype of BM early B and pro-B cells were mobilized into the PB (*B*).

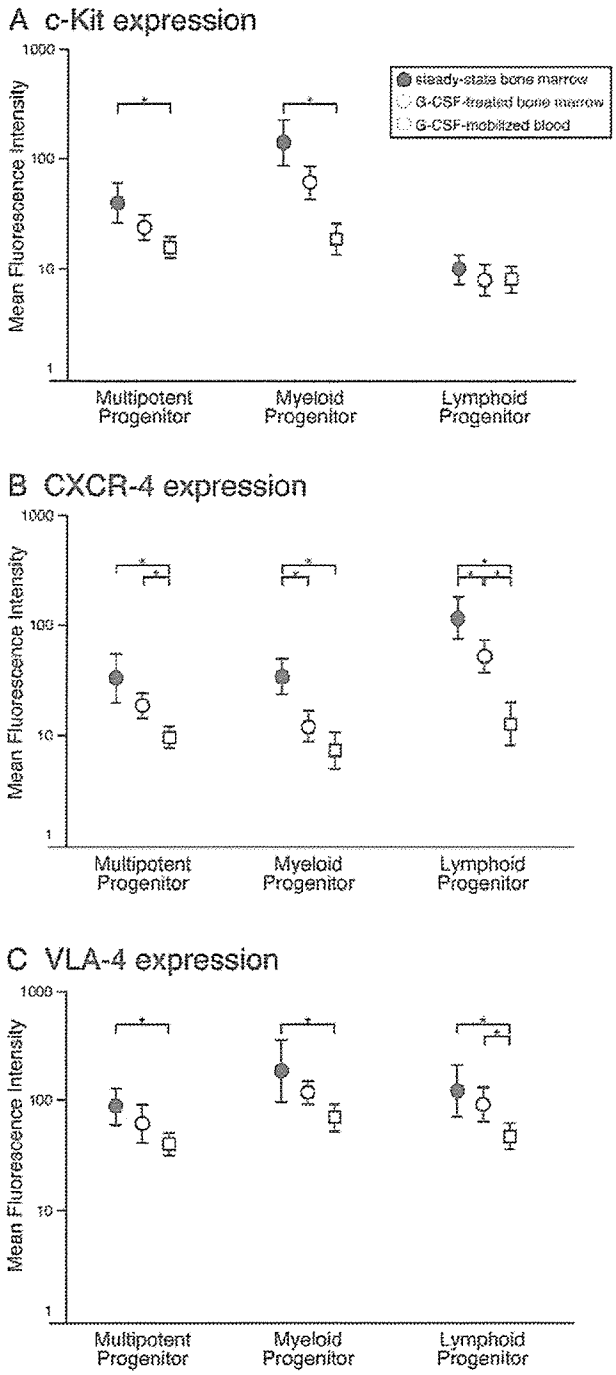

FIGURE 2. Comparative expression of c-Kit (*A*), VLA-4 (*B*), and CXCR-4 (*C*) on $CD34^+CD38^{-/low}Lin^-$ multipotent progenitors, $CD34^+CD38^+CD13^+$ myeloid progenitors, and $CD34^+CD38^+CD10^+$ lymphoid progenitors in the steady-state BM (●), G-CSF-treated BM (○), and G-CSF-mobilized PB (□). Circles and boxes indicate median MFI for these molecules among progenitors, and bars show SD. *, $p <$ **0.05, significantly different compared with each tissue.**

CXCR-4 and VLA-4 expression for all three progenitor types in BM declined after G-CSF administration; further decrease was observed in the G-CSF-mobilized progenitors. These results suggest that adhesion molecule expression on HPC in BM decreased during G-CSF administration in a lineage-independent manner. As a result, a fraction of cells with lesser expression of these molecules may be mobilized into the circulation.

Mobilized lymphoid cells are restricted to B/NK cell lineage

To test the differentiation capacity of mobilized cells possessing immature lymphoid phenotypes, doubly sorted $CD34^+CD10^+CD19^-$ and $CD34^+CD10^+CD19^+$ cells were cultured on methylcellulose with IL-7, SCF, IL-11, IL-3, GM-CSF, erythropoietin, thrombopoietin, and FL. One hundred $CD34^+Lin^-$ or $CD34^+CD38^+Lin^-$ cells purified from BM and G-CSF-mobilized PB gave rise to a variety of colonies including all types of myeloid lineages (13). In contrast, 500 $CD34^+CD10^+CD19^-$ and $CD34^+CD10^+CD19^+$ cells sorted from the steady-state BM and G-CSF-mobilized PB did not form any colonies after 14 days of culture under this condition (data not shown).

After 4 wk of culture on MS-5 or Sys-1 stromal layers in the presence of IL-7, SCF, IL-11, IL-3, IL-2, GM-CSF, and FL, BM $CD34^+Lin^-$ cells differentiated into $CD15^+$ myeloid cells, $CD19^+$ B lymphoid cells, and $CD56^+$ NK cells (Fig. 3, *A* and *B*). In contrast, early B cells sorted from BM and G-CSF-mobilized PB gave rise to $CD10^+CD19^+$ pro-B cells and $CD10^-CD19^+$ pre-B cells as well as NK cells but not myeloid cells (Fig. 3, *C*, *D*, *G*, and *H*). Pro-B cells from BM and G-CSF-mobilized PB also formed $CD19^+$ B cell-containing colonies, but neither myeloid nor NK cells were detected in cultured cells (Fig. 3, *E*, *F*, *I*, and *J*). Production of T cells was not observed in any of these cultures (data not shown).

Six to 8 wk after transplantation of FACS-sorted progenitors into irradiated NOD/SCID/$\beta2^{-/-}$ mice, animals were sacrificed to assess reconstitution of human hematopoiesis. FACS analysis of spleen and BM cells showed the presence of human $CD45^+$ cells in all mice transplanted with 50,000 $CD34^+Lin^-$ cells, $CD34^+CD38^+CD10^-CD19^+Lin^-$ pro-B cells, and $CD34^+CD38^+CD10^+Lin^-$ cells (including early B and pro-B cells). Strikingly, mice transplanted with $CD34^+CD38^+CD10^+Lin^-$ cells exhibited massive splenomegaly (5- to 10-fold enlargement) in contrast to mice receiving $CD34^+Lin^-$ cells, indicating that lineage-committed B lymphoid progenitors might proliferate rapidly in the spleen. In mice receiving human $CD34^+Lin^-$ cells, most $CD45^+$ cells in the spleen and BM were positive for CD19 (68 ± 7% and 45 ± 14%, respectively), but $CD45^+CD15^+$ and $CD45^+CD56^+$ cells also were found in both spleen and BM; thus, human $CD34^+Lin^-$ cells could differentiate into myeloid cells, B cells, and NK cells in these mice (Fig. 4*A*). In contrast, mice transplanted with 50,000 pro-B cells sorted from BM or G-CSF-mobilized PB exhibited only B lymphoid reconstitution (Fig. 4*B*). However, human $CD45^+$ cells could not be detected in animals transplanted with up to 3000 $CD34^+CD38^+CD10^+CD19^-Lin^-$ early B cells: the number of injected early B cells might not be sufficient to engraft mice. Because early B cell population was too tiny to sort cells enough for engraftment in xenogeneic hosts, we tested the differentiation potential of early B cells in vivo by injecting $CD34^+CD38^+CD10^+Lin^-$ cells, containing both $CD19^-$ early B and $CD19^+$ pro-B cells. Mice transplanted with $CD34^+CD38^+CD10^+Lin^-$ cells sorted from BM or G-CSF-mobilized PB reconstituted both $CD19^+CD56^-CD15^-$ B cells and $CD19^-CD56^+CD15^-$ NK cells in the BM and spleen (Fig. 4*C*). These in vitro and in vivo data revealed that G-CSF-mobilized $CD34^+CD38^+CD10^+CD19^+$ and $CD34^+CD38^+CD10^-CD19^+$ cells can rapidly differentiate in a B/NK and B lineage-restricted manner, which represents the same functional properties as in their BM counterparts, early B and pro-B cells.

Lymphoid progenitors have no self-renewing capacity

To test limited self-renewal activity, BM and G-CSF-mobilized early B and pro-B cells were plated in limiting dilution in LTC-IC assays and transferred to methylcellulose after 6 wk of culture as described previously (13). The estimated frequency of LTC-IC

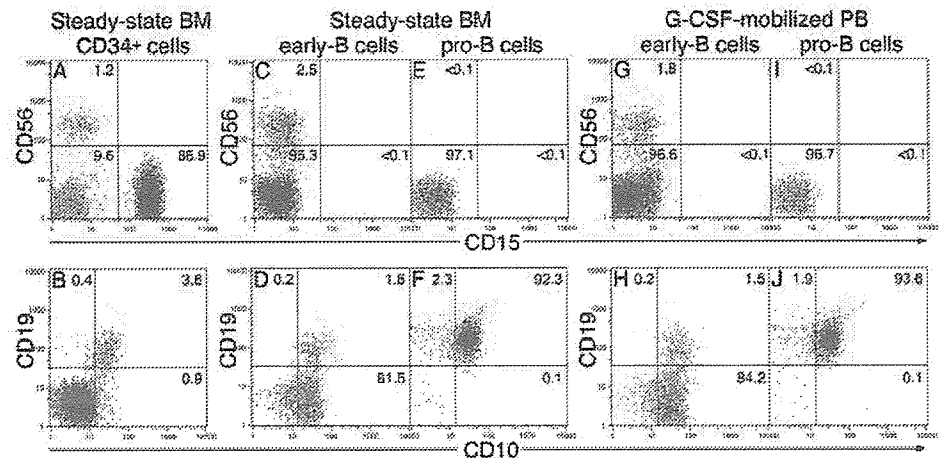

FIGURE 3. Differentiation potential of FACS-sorted progenitors in stroma-supported cultures. Cells cocultured on MS-5 and Sys-1 stromal cell layers with IL-7, SCF, IL-11, IL-3, IL-2, GM-CSF, and FL were harvested after 28 days, and FACS analysis was gated for viable CD45$^+$ cells. CD34$^+$Lin$^-$ BM cells differentiated into CD15$^+$ myeloid, CD56$^+$ NK cells (*A*), and CD10$^+$CD19$^-$ early B and CD10$^+$CD19$^+$ pro-B cells (*B*). Steady-state BM early B and pro-B cells gave rise to more differentiated lymphoid-restricted cells such as CD10$^+$CD19$^+$ pro-B and CD10$^-$CD19$^+$ pre-B cells and CD56$^+$ NK cells, but not myeloid cells (*C–F*). Similarly, CD10$^+$CD19$^-$ and CD10$^+$CD19$^+$ cells sorted from G-CSF-mobilized PB possessed B lymphoid-restricted differentiation potential in the stromal cell cultures (*G–J*).

was 1 in 20 for CD34$^+$CD38$^-$Lin$^-$ cells, but no LTC-IC activity was detected in early B and pro-B cells from either BM or G-CSF-mobilized PB (data not shown).

Differentiation potential of early B cells in limiting dilution analysis

We next evaluated B cell differentiation capacity of BM and G-CSF-mobilized early B cells at limiting dilution in culture on MS-5 stromal cell layers, which can support differentiation of B lymphoid progenitors from human CD34$^+$ cells (15). As shown in Fig. 3, early B cells were capable of differentiation into CD10$^+$CD19$^+$ pro-B cells and CD10$^-$CD19$^+$ pre-B cells after 4 wk of culture under this condition. In a limiting dilution assay, we estimated that one in eight BM early B cells and one in 10 G-CSF-mobilized early B cells could read out B cell differentiation in this culture condition (Fig. 5). Frequency of B cell development did not differ significantly between BM and G-CSF-mobilized early B cells.

Mobilized lymphoid progenitors show lineage-specific gene expression profiles

We tested expression of several genes in early B and pro-B cells sorted from the G-CSF-mobilized PB and BM by RT-PCR. Lymphoid lineage-specific genes such as IL-7R, TdT, Pax-5, and VpreB were expressed in early B and pro-B cells from both BM and G-CSF-mobilized PB (Fig. 6). Granulocyte lineage-related genes including G-CSFR, GM-CSF receptor, and myeloperoxidase were not detected in early B or pro-B cells from either BM or G-CSF-mobilized PB (Fig. 6).

IgH rearrangement in G-CSF-mobilized B lymphoid progenitors

We examined the IgH rearrangement status in the mobilized B lymphoid progenitors, because Ig genes rearrangement status reflect well the differential stages in the B cell development pathway. In general, along with B cell differentiation pathway, Ig genes rearrangements proceed from DJ_H at the early B cells or CLP stage through VDJ_H at the pro-B cells stage and to L chain gene at the pre-B cells stage (17, 20, 23, 24).

In our experiments, DJ_H and VDJ_H rearrangements were undetectable in the most immature CD34$^+$CD38$^-$Lin$^-$ cells sorted from both BM and the G-CSF-mobilized PBPC. In contrast, a ladder of DJ_H rearrangement bands ranging from 70 bp to 100 bp was observed in BM and G-CSF-mobilized CD34$^+$CD10$^+$CD19$^-$ early B cells (Fig. 7). VDJ_H and DJ_H rearrangements were detected in both BM and G-CSF-mobilized CD34$^+$CD10$^+$CD19$^+$ pro-B cells. The mobilized B lymphoid progenitors undergo IgH gene rearrangements in parallel with their BM counterparts.

Discussion

In this study, using multicolor flow cytometry, we demonstrated that administration of G-CSF to human subjects induced mobilization into PB of tiny but significant cell populations possessing the same immature lymphoid phenotypes as those of B/NK and B lymphoid-committed progenitors that are well defined in the BM. These populations are phenotypically identified as CD34$^+$CD10$^+$CD19$^-$Lin$^-$ early B cells (or CLP) and CD34$^+$CD10$^+$CD19$^+$Lin$^-$ pro-B cells and do not circulate in PB under steady-state condition (14, 20). Importantly, however, a phenotypically defined population of mobilized blood cells may not necessarily have the same functional properties as its BM counterpart. Mobilized CD34$^+$CD10$^+$CD19$^-$Lin$^-$ cells and CD34$^+$CD10$^+$CD19$^+$Lin$^-$ cells had prominent B/NK and B lymphoid differentiation potential in vivo and in vitro, respectively. Neither of these two populations exhibited self-renewal or LTC-IC capacity, indicating that the mobilized cells had characteristics of B/NK and B lineage-committed progenitors. In addition, in a limiting dilution assay, the mobilized cells had a differentiation potential for B/NK lymphoid lineage equivalent to that of BM early B cells. Furthermore, mobilized B lymphoid progenitors expressed only B lymphoid lineage-affiliated genes, with no expression of myeloid-lineage restricted genes including G-CSFR. IgH genes rearrangements were detected in early B cells and pro-B cells sorted from the G-CSF-mobilized PBPC, respectively. Collectively, these results demonstrate that a phenotypically defined lymphoid progenitor in the G-CSF-mobilized PB had the same functional properties as its BM counterpart, indicating that BM-resident B lymphoid progenitors could be released into the periphery by administration of G-CSF.

HPC express various molecules such as VLA-4/VCAM-1, SDF-1/CXCR-4, and Kit-ligand, and anchor to the BM through adhesive contact with their respective ligands in the BM microenvironment. Several studies have demonstrated that following G-CSF

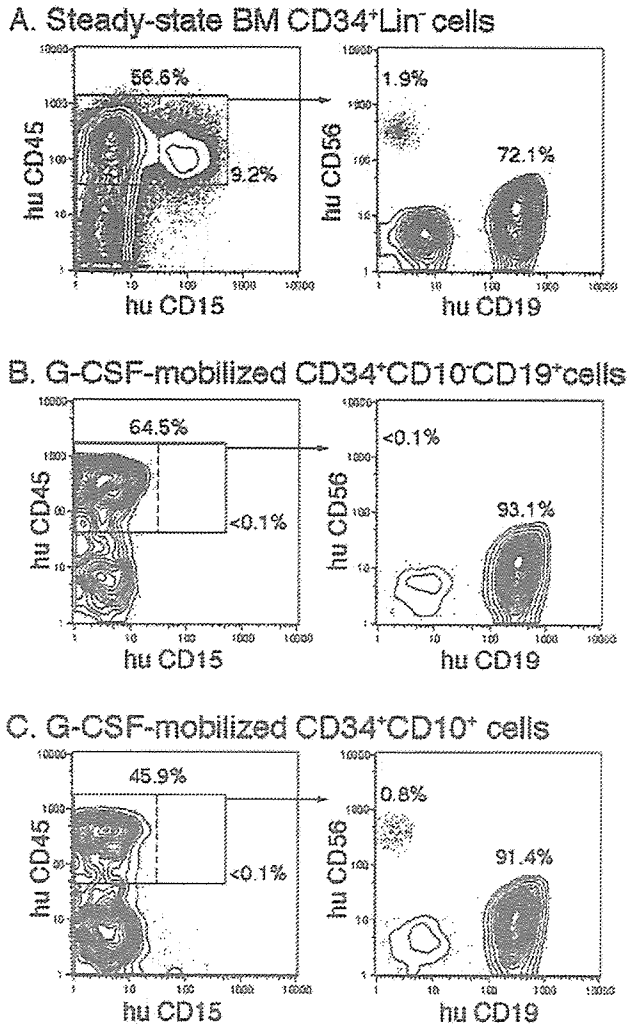

FIGURE 4. Engraftment and reconstitution potential of human different progenitors in NOD/SCID/$\beta2^{-/-}$ mice. Six to 8 wk after i.v. injection of 50,000 $CD34^+Lin^-$ cells, $CD34^+CD38^+CD10^-CD19^+Lin^-$ pro-B cells, and $CD34^+CD38^+CD10^+Lin^-$ cells (including early B and pro-B cells) into irradiated mice, analysis was gated for viable human $CD45^+$ cells. Human $CD15^+$ myeloid, $CD56^+$ NK, and $CD19^+$ B cells were detected in the mice transplanted with BM $CD34^+Lin^-$ cells (*A*). In contrast, only B cells were generated in mice transplanted with G-CSF-mobilized $CD34^+CD38^+CD10^-CD19^+$ cells (*B*). Mice transplanted with $CD34^+CD38^+CD10^+Lin^-$ cells reconstituted both B and NK cells (*C*). Representative analyses of mice BM are shown.

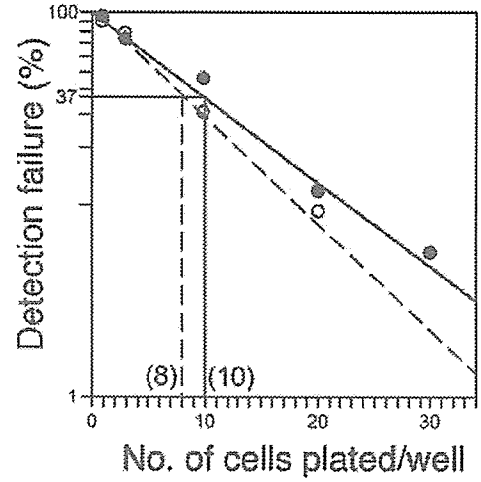

FIGURE 5. Limiting dilution analysis of early B cells from steady-state BM and G-CSF-mobilized PB. $CD34^+CD38^+CD10^+CD19^-$ cells plated by limiting dilution on MS-5 stromal layers were cultured in the presence of IL-7, IL-2, IL-11, SCF, and FL for 28 days. The differentiation potential of cells in individual wells was determined as $CD19^+$ mature B cells as shown in Fig. 3, *D* and *H*. We estimated that one in eight BM early B cells (○) and one in 10 G-CSF-mobilized $CD10^+CD19^-$ cells (●) could undergo B cell differentiation under this condition, indicating that G-CSF-mobilized $CD10^+CD19^-$ cells possess the same B cell differentiation potential as early B cells from BM. Numbers in parentheses represent limiting numbers.

administration, activated neutrophils and monocytes release proteolytic enzymes such as neutrophil elastase, cathepsin G, and MMP-9, which cleave and/or inactivate adhesion molecules expressed on the HPC (25–31). In fact, decreased expression of VLA-4 (32–35), CXCR-4 (28, 36), and c-Kit (30, 37, 38) on mobilized HPC has been reported during G-CSF administration in humans. Altered expression of adhesion molecules and consequent modification of their adhesion capacity might lead to release and migration of HPC into the circulation (7–11). Our study showed decreased expression of VLA-4 and CXCR-4 on circulating progenitors including MPP, myeloid, and lymphoid progenitors following G-CSF administration compared with that of BM, suggesting possible involvement of adhesion molecules in mobilization of at least three different types of immature progenitors. However, the extent to which each of these molecules contributed to mobilization of each hemopoietic lineage (11), or whether specific adhesion molecules are modulated in a lineage-dependent fashion, was not clear. Among the adhesion molecules that we examined, a dramatic decrease was observed in CXCR-4 expression on the lymphoid progenitors mobilized by G-CSF administration. SDF-1/CXCR-4 interactions also are involved in B lymphopoiesis, as substantiated by studies in CXCR-4-deficient mice that demonstrated reduced numbers of B lymphoid progenitors in the BM but abnormally high numbers of B lymphoid progenitors as well as the presence of mature B cells in blood and spleen (22, 39, 40). This suggests that CXCR-4 is required to retain B lymphoid progenitors within BM microenvironment for further maturation, as opposed to direct signaling to promote B cell development. These results agree with our findings that despite reduced expression in CXCR-4, the same differentiation capacity was preserved in mobilized lymphoid progenitors as their counterparts had in the steady-state BM. Thus, a decrease in CXCR-4 expression could be induced in a lineage-independent fashion following G-CSF, with resulting modulations contributing to migration of HPC without loss or alteration of differentiation capacity.

Importantly, hemopoietic growth factors can affect growth and/or properties of hemopoietic progenitors and cells. G-CSF has been characterized as a pivotal cytokine in proliferation, maturation, and survival in the myeloid lineage development pathway. Thus, G-CSF may affect potential or manifest characteristics of HPC during G-CSF mobilization, and HPC may have different abilities to develop and function. For example, mobilized $CD34^+$ cells have been reported to show decreased cell cycling compared with their BM counterparts (38, 41). In addition, numerous recent studies have demonstrated differentiation plasticity of committed progenitors, suggesting that hemopoietic progenitors retain a latent *trans* differentiation potential making them susceptible to diversion from their developmental fate (42–46). These observations suggest that circulating B lymphoid progenitors exposed to extremely high concentrations of G-CSF might show a different potential